Unnatural evolutionary processes of SARS-CoV-2 variants and possibility of deliberate natural selection

Atsushi Tanaka[1,2,*] †, Takayuki Miyazawa[2,3,*] †

[1]Division of Research Animal Laboratory and Translational Medicine, Research and Development Center Osaka Medical and Pharmaceutical University, Takatsuki, Osaka 569-8686, Japan

[2]Laboratory of Virus-Host Coevolution, Institute for Life and Medical Sciences, Kyoto University, Sakyo-ku, Kyoto 606-8507, Japan

[3)] Resilience Research Unit, Kyoto University, Katsura, Nishikyo-ku, Kyoto 615-8540, Japan

*** Correspondence:**
Atsushi Tanaka*****
atsushi.tanaka@ompu.ac.jp

Takayuki Miyazawa*****
takavet@infront.kyoto-u.ac.jp

Keywords: SARS-CoV-2, evolution, Omicron BA.1, Omicron BA.2, SARS-CoV-2 Omicron, Puerto Rico.

Abstract

Over the past three years, severe acute respiratory syndrome coronavirus 2 (SARS-CoV-2) has repeatedly caused pandemics, generating various mutated variants ranging from Alpha to Omicron. In this study, we aimed to clarify the evolutionary processes leading to the formation of SARS-CoV-2 Omicron variants, focusing on Omicron variants with many amino acid mutations in the spike protein among SARS-CoV-2 isolates. To determine the order of mutations leading to the formation of the SARS-CoV-2 Omicron variants, we compared the sequences of 129 Omicron BA.1-related, 141 BA.1.1-related, and 122 BA.2-related isolates, and attempted to clarify the evolutionary processes of SARS-CoV-2 Omicron variants, including the order of mutations leading to their formation and the occurrence of homologous recombination. As a result, we concluded that the formation of a part of Omicron isolates BA.1, BA.1.1, and BA.2 was not the product of genome evolution, as is commonly observed in nature, such as the accumulation of mutations and homologous recombinations. Furthermore, the study of 35 recombinant isolates of Omicron variants BA.1 and BA.2 confirmed that Omicron variants were already present in 2020. The analysis showed that Omicron variants were formed by an entirely new mechanism that cannot be explained by previous biology, and knowing how the SARS-CoV-2 variants were formed prompts a reconsideration of the SARS-CoV-2 pandemic.

1 Introduction

COVID-19, the coronavirus disease 2019, caused by severe acute respiratory syndrome coronavirus 2 (SARS-CoV-2), was first reported in December 2019 in Wuhan, China (1). This emerging infectious disease was unprecedentedly fast, spreading worldwide, leading the World Health Organization (WHO) to declare a global pandemic of COVID-19 on March 11, 2020 (https://www.who.int/). SARS-CoV-2, belonging to betacoronavirus subgroup B, has a single-stranded positive-sense RNA genome that codes for ten genes, ultimately producing 26 proteins according to an annotation of NCBI Reference Sequence: NC_045512.2. Its genome size varies from 29.8 to 29.9 kb. It consists of four structural proteins: spike (S), envelope (E), membrane (M), and nucleocapsid (N) proteins (2, 3). In the structural proteins, the S protein as the surface glycoprotein is the largest protein, being approximately 180 kDa, and consisting of two subunits, S1 and S2. It mediates membrane fusion and ultimately facilitates virus entry. The receptor-binding domain (RBD) (amino

acid residues 319‑541) of the S1 subunit interacts with angiotensin‑converting enzyme 2 (ACE2), binding to its peptidase domain (4, 5).

Over the three years from 2019 to 2022, SARS-CoV-2 was re-accelerated by new variants that emerged over several months in various geographical regions and disseminated throughout the world, to induce the pandemic repeatedly.

In the early stage of the first pandemic, the most impactful mutation of SARS-CoV-2 was the non-synonymous mutation D614G in the S protein. This mutation, which was not present in the ancestral lineage that caused the Wuhan outbreak, quickly became dominant worldwide (6). Soon after, the variant of concern, B.1.1.7 : 20I (Alpha, V1), the lineage B.1.1.7 (clade 501.YV1), or Alpha, characterized by 17 unique mutations containing ten amino acid differences in the S protein, was first detected in southeastern England in late September 2020 (7) and expanded rapidly across the United Kingdom to become predominant during early 2021, spreading to most European countries with similar success. By November 2021, local transmission of this lineage had been reported in 175 countries (8). Shortly after, the emergence of variant strains of SARS-CoV-2 Alpha, variants B.1.351 : 20H (Beta, V2), was identified in October 2020, which was first detected in the Eastern Cape province of South Africa from specimens collected in early August. This Beta variant spread within South Africa and was considered to have displaced the other SARS-CoV-2 lineages circulating there (9). Then, the variant P.1: 20J (Gamma, V3) was identified in Brazil in December 2020, thought to have evolved in Brazil. Health officials in Japan first reported it publicly on January 10, 2021, after identifying the Gamma variant in four Brazilian travelers at Haneda Airport in Tokyo, Japan (10).
At about the same time, the Delta variant (Pango lineage designation B.1.617.2), which was first detected in India in February 2021, and the Mu variant, also known as lineage B.1.621 first detected in Colombia in January 2021, were reported (11, 12). While the lambda variant (Pango lineage designation C.37), was detected in Peru in August 2020, but designated in June 15, 2021 by WHO (13, 14).

Almost one year later, regarding these emergences of variants of concern, Omicron (phylogenetic assignment of named global outbreak (Pango) lineage designation B.1.1.529; BA.1, Nextstrain clade 21K) was a variant of SARS-CoV-2 first reported to WHO by the Network for Genomics Surveillance in South Africa on November 24, 2021 (15, 16) with more than 50 amino acids changes when compared with the first reported strain Wuhan-Hu-H1 (NCBI Reference Sequence: NC_045512.2.), and 39 of these amino acids difference were observed in the S protein. This variant was first detected in Botswana and became the predominant circulating variant worldwide (17).

In the United States, the San Francisco Department of Public Health confirmed that a case of COVID-19 among individuals in California was caused by Omicron variant BA.1, carried by a traveler who returned from South Africa on November 22, 2021 (https://www.cdc.gov/media/releases/2021/s1201-Omicron-variant.html). Then, the first Omicron sub-lineage BA.1 expanded rapidly and replaced the Delta variant (18).

Less than two weeks later, the Omicron variant BA.1, the new Omicron variant, BA.2 lineage, showing 31 amino acids changes in the S protein when compared with the Wuhan-Hu-H1, was initially identified in Denmark on December 5, 2021 (19). On February 22, 2022, WHO mentioned the Omicron sublineage BA.2 (https://www.who.int/news/item/22-02-2022-statement-on-Omicron-sublineage-ba.2), whereby the Omicron variant of concern was currently the dominant variant circulating globally, replacing the Delta variant (Pango lineage designation B.1.617.2) (https://www.who.int/docs/default-source/coronaviruse/2022-01-07-global-technical-brief-and-priority-action-on-Omicron---corr2.pdf?sfvrsn=918b09d_20), accounting for nearly all sequences reported to GISAID. Then, as of March 16, 2023, WHO stated that the Omicron variants accounted for over 98% of the publicly available viral sequences after February 2022 (https://www.who.int/news/item/16-03-2023-statement-on-the-update-of-who-s-working-definitions-and-tracking-system-for-SARS-CoV-2-variants-of-concern-and-variants-of-interest).

Omicron variants BA.1 and BA.2 were suggested to have expanded and diverged around October to December 2021, respectively. These mutants were estimated to have diverged from a common ancestor around February to March 2021 (20). Since Omicron variants BA.1 and BA.2 share a common 14-amino acid mutation in the S

protein, the common ancestor of Omicron variants BA.1 and BA.2 may have already acquired the 14-amino acid mutation in the S protein region around February to March 2021; however, no common ancestral strain has been found in the international databases, and the strains may have acquired their mutations through different pathways.

In this study, we attempted to clarify the evolutionary processes of the Omicron variant, which has two-times more amino acid mutations in the S protein than other variants, by examining the rank order of introduced amino acid mutations in the S protein.

2 Results

Each variant is considered to have arisen through an independent evolutionary pathway from isolates with the D614G mutation in the S protein. Concerning the genetic variation in the S protein of these variants, most of the mutations were non-synonymous (Fig. 1). There were no synonymous mutations in the Alpha, Beta, Gamma, Delta, or Mu variants, but only one each in the Lambda and Omicron variants. Among these variants, the Omicron variant (BA.1 lineage), which shows the greatest accumulation of mutations in the S protein, is primarily non-synonymous in the S protein and has only one synonymous mutation, at c25000u. The synonymous/non-synonymous ratio is abnormal, considering how human coronaviruses have mutated (See Supplemental Figure 1).

At first, we considered the existence of the isolate of SARS-CoV-2, whose amino acid sequence in the S protein contains the Omicron-BA.1-type mutation subsets, but one mutation position was not mutated and comprised the original Wuhan-type amino acid sequence. We designated these isolates as BA.1-01. Each amino acid sequence of the S protein region was named BA.1-0.1_S: amino acids of the Omicron-BA.1 type (Oaa) and Wuhan type (Waa) and its position number (XXX) (Ex., BA.1-0.1_S:OaaXXXWaa), as described in Methods. Then, the putative isolates bearing BA.1-0.1_S:OaaXXXWaa were searched for using the BLAST program based on their amino acid sequences. In this search, we obtained the isolates whose identities showed 100% matches with the query amino acid sequence except for SARS-CoV-2_human_USA_NY-PV55373_2022(GenBank: ON246090.1), whose identity was 99.92%.

Surprisingly, we found that Omicron BA.1-0.1 isolates were detected at all mutation sites except N501Y (Fig. 2A). In the BA.1 lineage of the Omicron variant, there are Omicron isolates (BA.1.1) with the R346K mutation seen in the Mu(m) variant (termed B.1.621), *i.e.*, BA.1_S can be defined as BA.1.1_S:K346R. We also performed a BLAST search for isolates with amino acid sequences of BA.1-0.1.1_S:OaaXXXWaa, as described in Methods. As a result, Omicron BA.1.1-subset-0.1 isolates were detected at all mutation sites except S373P (Fig. 2B). Similar to the BA.1 lineage of the Omicron variant, in the BA.2 lineage of the Omicron variant, isolates of BA.2-0.1 were found at all mutant sites except T478K and P681H in the S protein (Supplemental Figure 2). The presence of these isolates refutes the establishment of Omicron strains through a continuous evolutionary process by accumulating mutations. So, we could not determine which mutation occurred first or last to form the Omicron variants. As shown in Fig. 2B, over half of the BA.1.1-0.1 isolates have the synonymous mutation c21595u detected in the S protein. However, this does not help explain the order in which the c21595u mutation arose. Curiously, in BA.1 strain isolates, this c21595u mutation was only detected in SARS-CoV-2_human_USA_ID-CDC-LC0481844_2022 (GenBank: OM409228.1) and SARS-CoV-2_human_USA_MI-CDC- ASC210597972_2022 (GenBank: OM396816.1). These isolates commonly lack the G339D mutation. This synonymous mutation is in a mutation-prone hotspot location. Still, if the same mutation occurred independently in different isolates, it is highly unnatural for the proportion of c21595u occurrences to be significantly biased in the Omicron variants BA.1.1-0.1.

It has been reported that two different variants were infected in a single cell while establishing various SARS-CoV-2 variants, causing homologous recombination in the process of viral RNA synthesis, resulting in multiple variants. On considering that homologous recombination caused the isolates shown in Fig. 2, some of the breakpoints at which strand changes occur by homologous recombination are too short (1nt, 2nt, 3nt, etc.) (Fig. 3 and Supplemental Figure 3). Therefore, it is unreasonable to employ homologous recombination as the basis for establishing these isolates. Also, most of these isolates were found in the USA between 2021 and 2022;

however, considering that the most prevalent variant in the USA in August 2021 was the Delta variant, it is most unlikely that it did not cause mutations such as T478K and D614G, which were already prevalent. It is inconceivable that the oldest variants (such as T478K and D614G), which were no longer prevalent, were sufficiently present to cause superinfection and be involved in homologous recombination. Also, most of these isolates were isolated in the USA between 2021 and 2022. Still, given that the isolates primarily prevalent in the USA in August 2021 were Delta variants, it is unlikely that an older type of variant without the T478K or D614G mutation was present to cause superinfection and be involved in homologous recombination. This consideration is supported by the fact that all of these BA.1-0.1 and BA.1.1-0.1 isolates retained the sequence of the BA.1 lineage in all regions except the S protein (Fig. 4). In addition, the fact that all of these BA.1-0.1 and BA.1.1-0.1 strains retained the sequence of Omicron strain BA.1 except for the S protein also makes it unreasonable to consider that these isolates arose by homologous recombination with an older type of mutant without the T478K or D614G mutations (Fig. 4).

Furthermore, some of the BA.1 and BA.1-0.1 isolates have mutation subsets (synonymous: u10135c, ORF3: L106F, N: D343G) up- and downstream of the S gene, and the u10135c and L106F (ORF3) mutations correspond perfectly. Therefore, it is considered that homologous recombination between the BA.1 variant and variants without these mutations did not occur during the mutants' formation processes (Fig. 4). The synonymous mutation c2470u occurred in BA.1.1 compared with BA.1, and this c2470u mutation was retained by most, excluding a few of the BA.1.1-0.1 isolates (SARS-CoV-2_human_USA_IL-CDC-ASC210695497_2022 : GenBank: OM770362.1; SARS-CoV-2_human_USA_NY-CDC-LC0450936_2021: GenBank: OM228453.1）. The synonymous mutation c2470u has also only been observed in a minimal number of BA.1-0.1 isolates （ SARS-CoV-2_human_USA_OR-CDC-LC0470830_2022: GenBank: OM367679.1; SARS-CoV-2_human_USA_ID-CDC-LC0481844_2022: GenBank: OM409228.1; SARS-CoV-2_human_USA_MI-CDC-ASC210597972_2022: GenBank:OM396816.1; SARS-CoV-2_human_USA_WI-CDC-LC0494047_2022: GenBank: OM500517.1）. These results suggest that the establishment of BA.1-0.1 and BA.1.1-0.1 isolates occurred independently. On the other hand, if reversion mutations caused each of these isolates with one amino acid different to the Wuhan-type, these isolates could be detected by examining an astronomical number of isolates. However, these virus strains were detected in the number of sequenced whole genomes (a limited number), rather than in astronomical numbers examined. The fact that most of these mutations occurred without synonymous mutations (Fig. 2) suggests that none of them arose as a result of trial-and-error random mutations in nature. Few synonymous mutations are detected in some BA.1-0.1, BA.1.1-0.1, and BA.2-0.1 isolates (Fig. 2 and Supplemental Figure 2), as seen in other viruses (Supplemental Figure 1). The c25000u is the only synonymous mutation that did not occur until BA.1, BA.1.1, BA.2, BA.1-0.1 BA.1.1-0.1, and BA.2-0.1 isolates were formed and was not observed in previous variants such as alpha, beta, gamma, delta, etc. Nevertheless, it is curious to find the occurrence of mutants with synonymous mutations such as c22120u, c24034u, c23635u, c24448u, c21811u, a23884g, c22987u, c23609a, c23413u, c23896u, c22879u, u24097a, c23893u, c24442u, u24847c, c24382u, c22264u, c22879u, c22480u, u21976c, c22480u, g24577a, and u23101c in BA.1.1, BA.1-0.1, and BA.1.1-0.1 isolates (Fig. 2 Synonymous Others), and a22948g, c23635u, c21859u, c22945u, c23701u, c22987u, a24433g, c23347u, u24640c, a24619g, c24865u, a23989g, u23047c, u24346c, c21811u, c21952u, a22753u, c23635u, c24023u, c24382u, and c22572u in BA.2-0.1 isolates (Supplemental Figure 2 Synonymous Others) after the formation of mutants with these subsets.

Although the only bias in our isolates collection, was only selection of isolates whose identities showed 100% matches with the query amino acid sequence in the BLAST search, these curious tendencies were observed is very interesting.

If two different viral variants infect a single cell simultaneously in the process of establishing various SARS-CoV-2 variants, and if homologous recombination occurs during viral RNA synthesis between the Omicron variant BA.1 lineage and BA.2 lineage, it is expected that there are variants caused by homologous recombination between the BA.1 and BA.2 lineages.

Therefore, we also performed BLAST searches for isolates with mutant amino acid subsets of both the Omicron variant BA.1 and BA.2 strains. We detected recombinant isolates of Omicron BA.1 and BA.2 lineages.

Surprisingly, the recombinant Omicron BA.1 and BA.2 lineages, SARS-CoV-2/human/PRI/PR-PR-UPRRP-582/2020 (GenBank: ON928946.1), were already present in Puerto Rico in 2020. Omicron (B.1.1.529) is a variant of SARS-CoV-2 first reported to WHO by the Network for Genomics Surveillance in South Africa on November 24, 2021 (15, 16). It was first detected in Botswana and spread to become the predominant variant in circulation worldwide (17). Following the appearance of the original B.1.1.529 variant, several subvariants of Omicron emerged, including BA.1, BA.2, BA.3, BA.4, and BA.5 (21). After October 2022, two subvariants of BA.5 called BQ.1 and BQ.1.1 emerged.

The question then arose about why a recombinant strain, SARS-CoV-2/human/PRI/PR-UPRRP-582/2020 (GenBank: ON928946.1), already existed in 2020. We searched for SARS-CoV-2 isolates prevalent in Puerto Rico using the keywords "PRI", "PR-UPRRP", and "2020" in the NCBI search; nucleotide (https://www.ncbi.nlm.nih.gov/). Consequently, we found 29 Omicron-associated sequences in the 127 hits obtained (Fig. 5B). These results suggest that the SARS-CoV-2 variants bearing the amino acid sequences of the S protein are identical to Omicron BA.1 and Omicron BA.2 variants, which were already prevalent in Puerto Rico in 2020, with 15 isolates showing the complete Omicron BA.1+ R346K_mut-subset (BA1.1) , and 14 isolates showing a synonymous substitution of c21595u. Four isolates had an amino acid sequence of the S protein that perfectly matched that of Omicron BA2 (BA.2_S), four isolates were Omicron BA.2-0.1 (BA.2-S:K440N) and four isolates were Omicron BA.2-0.1 (BA.2-S:K440N)+F79S, BA.2-0.1 (BA.2-S:K440N)+Q613H, BA.2-0.1 (BA.2-S:K440N)+212S+D215E and BA.2-0.1 (BA.2-S:K440N)+212S (Fig. 5B).

3 Discussion

Several hypotheses have been proposed in which the original SARS-CoV-2 virus resulted from an accidental laboratory spill. With recent developments in biotechnology, many viruses, including coronaviruses, have been artificially synthesized and used in various experiments (22-24). The artificial generation of mutant viruses in laboratories and study of viral phenotypes by introducing mutations is called "reverse genetics", being a common technique in virology. It has been claimed that SARS-CoV-2 must have been artificially generated because of the unnatural presence of a codon (CGG) encoding a contiguous arginine at the furin cleavage site of SARS-CoV-2. This claim has been refuted based on the following facts: 1) there is no logical reason for a genetically engineered virus to utilize such a suboptimal furin cleavage site; 2) The only previous study on artificial insertion of furin cleavage sites at the S1/S2 boundary of the S protein of SARS-CoV-1 using the pseudotype virus experimental system utilized the optimal "RRSRR" sequence, which is different from the furin cleavage site's sequence present in SARS-CoV-2; 3) There is no evidence of previous studies at the Wuhan Institute of Virology that artificially inserted a complete furin cleavage site in coronaviruses; 4) Unnatural CGG codons adjacent to arginine at the furin cleavage site are rare in coronaviruses but are observed at a particular frequency in SARS-CoV-1, SARS-CoV-2, and other human coronaviruses. However, these are only declarations and are not logical. No one has offered an explanation why a naturally occurring virus would utilize a suboptimal furin cleavage site. There has been no mention of the technical possibility of inserting this furin cleavage site or a CGG codon artificially. The insertion of a polybasic furin cleavage site into the S protein makes it impossible to conclude whether SARS-CoV-2 is a naturally occurring or an artificial virus.

Despite the accumulation of many mutations in the S protein of Omicron mutants, most of the mutations are non-synonymous, with only one synonymous mutation of c25000u, which is highly unnatural, leading to the hypothesis that the Omicron mutants were artificially synthesized. The following results presented in this study may support the hypothesis that the Omicron variants were artificially synthesized rather than naturally occurring: 1) the presence of Omicron variant-associated isolates with one mutation site being the Wuhan-type; 2) the almost complete absence of synonymous mutations in the S protein in these isolates; 3) the Omicron variant, which should have been first reported to WHO from South Africa on November 24, 2021, was already endemic in Puerto Rico in 2020, and there were isolates that were recombinants between Omicron strains BA1 and BA2. In addition, the Omicron mutant-related isolates (BA.1-0.1, BA.1.1-0.1, and BA.2-0.1 isolates) with a Wuhan-type mutation at one of the mutation sites were established. Some had synonymous mutations after

establishing the Omicron mutant-related isolates (Fig. 2 and Supplemental Figure 2 Synonymous Others). It is reasonable to assume that viruses with the reversion amino acid mutations caused by non-synonymous mutations in the S protein were artificially synthesized and then acquired further synonymous mutations in the natural environment.

Assuming that artificially synthesized mutants with only non-synonymous mutations are spread globally, this would explain how mutants with non-synonymous mutations without previous synonymous mutations develop synonymous mutations under natural circumstances. Considering the current epidemic situation of SARS-CoV-2, it is unlikely that these viruses arose spontaneously. Based on our efforts to explain the formation of the SARS-CoV-2 isolates, they were formed by a completely new mechanism that cannot be explained by previous biology.

One idea, the hypothesis that these viruses were artificially generated, is more reasonable than proposing a novel mutation acquisition mechanism. However, is there any reason to artificially create these mutants, which are unlikely to have occurred naturally, given the current SARS-CoV-2 epidemic?

It is known that the pathogenicity, host specificity, cell tropism, and immunogenicity of numerous viruses can be altered by mutation of a single (or several) amino acid(s) of a viral protein on the viral envelope (envelope protein, HA protein, spike protein, etc.). A single-amino-acid substitution in the HA protein of the 2009 pandemic A (H1N1) influenza viruses changed their replication and pathogenicity (25). In the Chikungunya virus, single amino acid changes in the E2 glycoprotein influenced glycosaminoglycan utilization for target-cell binding (26), and a single amino acid change in the E1 glycoprotein affected mosquito vector specificity and epidemic potential (27). In previous coronaviruses such as MERS-CoV and SARS-CoV-1, point mutations have been demonstrated to confer resistance to neutralizing antibodies (28-30).

Consider that the SARS-CoV-2 Omicron variant and its one-amino-acid reversion mutants were artificially and systematically generated. In that case, we should suspect that the other variants (Alpha to Delta) were also artificially generated viruses. Indeed, the lack of findings to date that many of the various mutations seen, especially in the early variants, are indeed associated with increased viral infection (31) supports the hypothesis that each variant was artificially synthesized to identify the amino acids of the S protein responsible for infectivity and pathogenicity. The possibility that the set of mutants was artificially generated to identify amino acids of the S protein involved in the infectivity and virulence is supported.

Reverse genetics experiments are an essential part of virus research, and it is inimical to virus research to consider that artificially synthesized viruses were deliberately spread throughout the world. However, now that reverse genetics has become common in virus research, we believe it is not scientific to discuss the mutation process of SARS-CoV-2 without excluding the possibility of artificially synthesized viruses.

Finally, we would like to add that while artificially synthesized viruses may have spread, we are not criticizing reverse genetics technology, as such technology has led to marked advances in virology. In addition, our analysis employed databases with a limited number of viral sequences, and we cannot deny the possibility that unreliable data may have been registered due to technical problems in sequencing or some other issues. Furthermore, we do not conclude that these viruses were artificially synthesized and distributed based on malicious intent. This study aims to point out that SARS-CoV-2 has undergone unthinkable mutations based on conventional coronavirus mutation mechanisms, and we hope that the possibility of artificial creation is included in serious discussions on the formation of SARS-CoV-2 variants.

Nonetheless, the analysis we have shown here concludes that the Omicron variants were formed by a completely new mechanism that cannot be explained by previous biology. The process of how SARS-CoV-2 mutations occurred should prompt a reconsideration of the SARS-CoV-2 pandemic. If the SARS-CoV-2 epidemic strain is an artificially mutated virus and if the corona disaster (corona hoopla) was a well-designed global experiment in human inoculation and a social experiment, then the design of this experiment and the nature of the virus used make it likely that this experiment (corona hoopla) is a preliminary experiment.

4 Methods

4.1 Data acquisition

The SARS-CoV-2 RNA genome, genes, and proteins according to an annotation of SARS-CoV-2 Wuhan-Hu-H1 (COVID-19/Wuhan-Hu-1CHN/2019/First Isolate) NCBI Reference Sequence: NC_045512.2 were used as references for the definition of mutations, and provided a basis for the numbering of nucleotides and amino acids of each protein. Genome data of SARS-CoV-2 isolates described in this article were obtained from the NCBI Nucleotide database (https://www.ncbi.nlm.nih.gov/) on 25/11/2022 to 17/03/2023.

4.2 Query of representative SARS-CoV-2 variant genome

Amino acid sequences of spike protein of SARS-CoV-2 variants（Alpha:B.1.1.7, Beta:B.1.351, Gamma:P1, Delta:B.1.617.2.63, Lambda:C.37, Mu:B.1.621, Omicron:BA.1, BA.1.1, and BA.2）were obtained from an Internet site, Stanford Coronavirus Antiviral & Resistance Database (https://covdb.stanford.edu/) or Covariant (https://covariants.org/), and used as a query sequence for an NCBI protein BLAST search (blastp: protein-protein BLAST, https://blast.ncbi.nlm.nih.gov/Blast.cgi?PROGRAM=blastp&PAGE_TYPE=BlastSearch&LINK_LOC=blasthome). Then, the whole genome sequence of each isolate bearing the query spike sequence was derived from the BLAST search result, identified with query amino acid sequences of 100%. The nucleotide sequences of the detected SARS-CoV-2 genome were as follows: GenBank Accession No.: GenBank: MW423686.2; MW430966.1; MW430967.1; MW422256.1; MW598419.1; MW667552.1; MW667553.1; MW721502.1; MW721504.1; MW520923.1; MW642248.1; MW642249.1; MW642250.1; MZ182066.1; MZ155303.1; MZ155230.1; MZ170364.1; MZ179869.1; MW666666.1; MW696612.1; MW699217.1; MW644498.1; MZ727706.1; MZ620161.1; MZ637380.1; MZ637401.1; MZ780550.1; OL672836.1; OL677199.1; OP769083.1; OL764360.1; OL815447.1; ON762438.1; OL849989.1; OL897126.1; OL896945.1; OL896936.1; OL896931.1; OM233931.1; OM072551.1; OM072822.1; OM296922.1.

4.3 Query of SARS-CoV-2 Omicron variant genome bearing an S protein amino acid sequence in which one of the Omicron-type nucleotide mutation subsets was not mutated and retains the original SARS-CoV-2 Wuhan-Hu-H1-type arrangement.

For each of the Omicron variants, BA.1, BA.1.1, and BA.2, the isolate series bearing an S protein amino acid sequence in which one of the Omicron-type nucleotide mutation subsets is not mutated and retains the original SARS-CoV-2 Wuhan-Hu-H1-type arrangement were named BA.1-0.1, BA.1.1-0.1 and BA.2-0.1, respectively. In addition, in this article, we named the amino acid sequences of spike protein of BA.1, BA.1.1, and BA.2 as BA.1_S, BA.1.1_S, and BA.2_S, respectively, and then the series of amino acid sequences of spike protein of BA.1-0.1, BA.1.1-0.1, and BA.2-0.1 were named, respectively, as follows: Omicron BA.1-0.1 spike series (BA.1-0.1_Ss) were named as BA.1_S:V67A; BA.1_S:69H_70V; BA.1_S:I95T; BA.1_S:D142G_143V_144Y_145Y; BA.1_S:I211N_212L; BA.1_S:ΔEPE; BA.1_S:D339G; BA.1_S:L371S; BA.1_S:P373S; BA.1_S:F375S; BA.1_S:N417K; BA.1_S:K440N; BA.1_S:S446G; BA.1_S:N477S; BA.1_S:K478T; BA.1_S:A484E; BA.1_S:R493Q; BA.1_S:S496G; BA.1_S:R498Q; BA.1_S:Y501N; BA.1_S:H505Y; BA.1_S:K547T; BA.1_S:G614D; BA.1_S:Y655H; BA.1_S:K679N; BA.1_S:H681P; BA.1_S:K764N; BA.1_S:Y796D; BA.1_S:K856N; BA.1_S:H954Q; BA.1_S:K969N and BA.1_S:F981L / Omicron BA.1.1-0.1 spike series (BA.1.1-0.1_Ss) were named as BA.1.1_S:V67A; BA.1.1_S:69H_70V; BA.1.1_S:I95T; BA.1.1_S:D142G_143V_144Y_145Y; BA.1.1_S:I211N_212L; BA.1.1_S:ΔEPE; BA.1.1_S:D339G; BA.1.1_S:L371S; BA.1.1_S:P373S; BA.1.1_S:F375S; BA.1.1_S:N417K; BA.1.1_S:K440N; BA.1.1_S:S446G; BA.1.1_S:N477S; BA.1.1_S:K478T; BA.1.1_S:A484E; BA.1.1_S:R493Q; BA.1.1_S:S496G; BA.1.1_S:R498Q; BA.1.1_S:Y501N; BA.1.1_S:H505Y; BA.1.1_S:K547T; BA.1.1_S:G614D; BA.1.1_S:Y655H; BA.1.1_S:K679N; BA.1.1_S:H681P; BA.1.1_S:K764N; BA.1.1_S:Y796D; BA.1.1_S:K856N; BA.1.1_S:H954Q; BA.1.1_S:K969N; BA.1.1_S:F981L / Omicron BA.2-0.1 spike series (BA.2-0.1_Ss) were named as BA.2_S:I19T;

BA.2_S:24L_25P_26P_S27A; BA.2_S:D142G; BA.2_S:V213G; BA.2_S:D339G; BA.2_S:F371S; BA.2_S:P373S; BA.2_S:F375S; BA.2_S:A376T; BA.2_S:N405D; BA.2_S:S408R; BA.2_S:N417K; BA.2_S:K440N; BA.2_S:N477S; BA.2_S:K478T; BA.2_S:A484E; BA.2_S:R493Q; BA.2_S:R498Q; BA.2_S:Y501N; BA.2_S:H505Y; BA.2_S:G614D; BA.2_S:Y655H; BA.2_S:K679N; BA.2_S:H681P; BA.2_S:K764N; BA.2_S:Y796D; BA.2_S:H954Q; BA.2_S:K969N, and these constructs are shown in Figs. 2, 4 and supplemental Figure 1. These amino acids sequences of spike protein of SARS-CoV-2 Omicron variants, BA.1-0.1, BA.1.1-0.1, and BA.2-0.1, were used as query sequences for an NCBI protein BLAST search. Then, the whole genome sequences of BA.1-0.1, BA.1.1-0.1, and BA.2-0.1 isolates bearing the query spike sequence were derived from the BLAST search results, identified with a query amino acid sequence of 100%. The nucleotide sequences of the detected SARS-CoV-2 genome were as follows: GenBank Accession No.: OM117411.1; OP797378.1; OM789835.1; OP928789.1; OP928803.1; OP929381.1; OP929396.1; OP929417.1; OM173977.1; OM518459.1; OM566981.1; ON019560.1; OM097227.1; OM096937.1; OM099902.1; OM117114.1; OM096685.1; OM354436.1; OM646886.1; OM472901.1; OM364511.1; OM131858.1; OL815451.1; OL896986.1; OL897116.1; OL897118.1; OL896964.1; OM367679.1; OM343778.1; OM409228.1; OM396816.1; OM134162.1; OM075886.1; OM123427.1; OM122677.1; OM121681.1; OM224850.1; ON246090.1; OM931599.1; OM864873.1; OM906519.1; OM906587.1; OM464776.1; OM015999.1; OM015958.1; OM015597.1; OM016329.1; OL898806.1; OL898861.1; OM016937.1; OM016186.1; OM036549.1; OM051171.1; OM126493.1; OM079115.1; OM099199.1; OM134489.1; OM098796.1; ON618279.1; ON618009.1; OM627701.1; OM356511.1; OM295457.1; ON700063.1; OM033824.1; ON368355.1; OM084700.1; ON208126.1; OM566593.1; OM945690.2; ON030252.1; ON019844.1; OM890075.1; ON020044.1; OM833954.1; ON376082.1; OM084604.1; OP795273.1; ON066609.1; OM352882.1; OM290510.1; OM369978.1; OM199342.1; OM011974.1; OM090274.1; OM043984.1; OM121683.1; OM121624.1; OM175506.1; OM360429.1; OM360221.1; OM358058.1; OM500517.1; OM135027.1; OM742858.1; OM521685.1; OM896558.1; ON694155.1; OM686755.1; OM484260.1; OM332056.1; OM156397.1; OM079447.1; OM134645.1; OM173298.1; OM123082.1; OM116023.1; OM652943.1; OL994299.1; OL994920.1; OM122027.1; OM121015.1; OL898817.1; OM527504.1; OM225320.1; OM931491.1; OM931575.1; OM931587.1; OM034409.1; OM036283.1; OL996129.1; OM035680.1; OM096996.1; ON065532.1; OM968098.1; OM816604.1; ON235452.1; ON334146.1; OP024162.1; OP209732.1; OM354578.1; OM099080.1; OM297301.1; OM297438.1; OM365368.1; OM449159.1; OM078863.1; OM096959.1; OM117155.1; OM133880.1; OM077358.1; OM372005.1; OM770362.1; OM897488.1; OM918459.1; OM918478.1; OL897115.1; OL897114.1; OL986779.1; OL986696.1; OL987046.1; ON831866.1; OM864099.1; OM863888.1; OP745925.1; ON831672.1; OM043643.1; OM176192.1; OM226685.1; OM343689.1; OM295527.1; OM894975.1; OM846676.1; OM822024.1; OM846844.1; OM906550.1; OM015933.1; OM016323.1; OM016331.1; OM035685.1; OM022498.1; OM156115.1; OM036875.1; OM099560.1; OM199246.1; OM067048.1; OM079299.1; OM099911.1; OM116588.1; OM097010.1; OM173300.1; OM805961.1; OM983266.1; OM983325.1; ON618010.1; OM084691.1; ON021265.1; ON039239.1; ON056981.1; ON144127.1; OM770527.1; OM156164.1; OM155119.1; OM199353.1; OM084630.1; OM084605.1; OM084621.1; OM359369.1; OM411574.1; OM584789.1; OM720486.1; OM429777.1; ON047062.1; ON065416.1; OP415118.1; OM954373.1; ON042406.1; OM335528.1; OM332335.1; OM353626.1; OM332813.1; OM197398.1; OM226919.1; OM228399.1; OM225859.1; OM271353.1; OM159454.1; OM224473.1; OM358278.1; OM361030.1; OM412141.1; OM496298.1; OM044048.1; OM121864.1; OM224477.1; OM227379.1; OM228453.1; OM622156.1; OM906370.1; OM970683.1; ON117965.1; OM198667.1; OM357800.1; OM357161.1; OM335230.1; OM261124.1; OM077578.1; OM497172.1; OM625194.1; OM907131.1; ON047464.1; OM911851.1; OM042846.1; OM155337.1; OM097339.1; OM116805.1; OM134409.1; OM686782.1; OM695863.1; OM724725.1; OM174366.1; OM822132.1; OM822106.1; OM822105.1; OM822485.1; OM135143.1; OM125829.1; OM098855.1; OM156118.1; OM155114.1; OM863926.1; OP359104.1; ON209298.1; ON232806.1; ON421981.1; ON811217.1; OM698275.1; ON052769.1; ON060006.1; ON060007.1; ON060009.1; OM843171.1; OM843276.1; OM843550.1; OM843316.1; OM843340.1; ON049267.1; ON450720.1; ON250163.1; ON256603.1; ON480422.1; OM888844.1; OM890089.1; ON009425.2; ON082904.1; OM901275.1; OM877094.2; OM877095.2; OM877096.2; OM877097.2; ON378542.1; ON389858.1; ON389889.1; ON390359.1; OM936703.1; ON352711.1; ON378000.1; ON177702.1; ON205494.1; ON378633.1; ON617689.1;

ON619375.1; OM567618.1; OM659585.1; OM770913.1; OM781641.1; OM533441.1; OM533458.1; OM570235.1; OM570252.1; OM570249.1; OM283361.1; OM283362.1; OM283320.1; OM283343.1; ON618014.1; ON618018.1; ON618019.1; ON618363.1; ON311615.1; ON383919.1; OP579158.1; OP054411.1; ON633107.1; ON414693.1; ON422887.1; OP364296.1; OP629673.1; ON363097.1; OP633561.1; ON458445.1; ON592247.1; ON549687.1; ON067040.1; ON321116.1; ON199452.1; ON200331.1; OM861064.1; OM969592.1; ON019120.1; ON221861.1; OM861619.1; ON091288.1; ON151370.1; ON233850.1; ON236456.1; ON296711.1; ON535443.1; ON624524.1; ON377450.1; ON397268.1; ON239032.1; ON373649.1; ON481637.1; ON701163.1; ON312677.1; ON349263.1; ON377487.1; ON377609.1; OM638574.1; OM911616.1; OM988767.1; ON019770.1; OM988769.1; ON468158.1; ON608924.1; ON604965.1; ON535763.1; ON378227.1; ON378238.1; ON728470.1.

4.4 Query of recombinant SARS-CoV-2 Omicron variant between BA.1 and BA.2 genome

Deduced recombinant spike protein between Omicron variants, BA.1 and BA.2 shown as BA.1_S:T19I_L24-_P25-_P26-_A27S_V213G_S371F_T376A_D405N_R408S was used as a query sequence for an NCBI protein BLAST search. The whole genome sequence of BA.1 and BA.2 recombinant-Omicron isolates showed some of the specific amino acid mutations observed in variant BA.1 and BA.2 in the S protein. The nucleotide sequences of the detected SARS-CoV-2 genome were as follows: GenBank Accession No.: OM360636.1; OM410816.1; OM429902.1; OM497964.1; OM565587.1; OM628132.1; ON549899.1; ON449685.1; ON176765.1; OM628094.1; ON099844.1; OM942313.1; ON395480.1; ON171854.1; ON172005.1; ON076710.1; ON928946.1; OM932113.1; OM942438.1; OM989528.1; OM499181.1; ON414822.1; OM878325.1; ON103067.1; ON103153.1; ON419036.1; ON928719.1; ON337887.1; ON420444.1; ON146520.1; OM469541.1; OM904085.1; ON254531.1; OM881098.1; ON373310.1.

4.5 Query of SARS-CoV-2 Omicron variant genome detected in Puerto Rico in 2020

Nucleotide sequences were searched using the keywords PRI PR-UPRRP 2020 (Search details: PRI[All Fields] AND (PR[All Fields] AND UPRRP[All Fields]) AND 2020[All Fields]). The search results were all SARS-CoV-2 isolate genome sequences. Among these sequences, SARS-CoV-2 Omicron variant-related sequences were picked up as follows: GenBank Accession No.: ON928761.1; ON928660.1; ON928794.1; ON928762.1; ON928848.1; ON928741.1; ON928918.1; ON928680.1; ON928975.1; ON928949.1; ON928673.1; ON928865.1; ON928716.1; ON928663.1; ON928779.1; ON928896.1; ON928946.1; ON928912.1; ON928704.1; ON928873.1; ON928813.1; ON928898.1; ON928765.1; ON928912.1; ON928883.1; ON928957.1; ON928880.1; ON928699.1; ON928724.1; ON928941.1.

Genomes were aligned using SnapGene software or GENETYX software. Numbering of nucleotides and amino acids of each protein was determined using Wuhan-Hu-1 (NC_045512.2; COVID-19/Wuhan-Hu-1CHN/2019/First Isolate) as a reference strain for the definition of mutations.

5. References

1. F. Wu, S. Zhao, B. Yu, Y. M. Chen, W. Wang, Z. G. Song, Y. Hu, Z. W. Tao, J. H. Tian, Y. Y. Pei, M. L. Yuan, Y. L. Zhang, F. H. Dai, Y. Liu, Q. M. Wang, J. J. Zheng, L. Xu, E. C. Holmes and Y. Z. Zhang: A new coronavirus associated with human respiratory disease in China. *Nature*, 579(7798), 265-269 (2020) doi:10.1038/s41586-020-2008-3
2. R. A. Khailany, M. Safdar and M. Ozaslan: Genomic characterization of a novel SARS-CoV-2. *Gene Rep*, 19, 100682 (2020) doi:10.1016/j.genrep.2020.100682
3. Y. M. Bar-On, A. Flamholz, R. Phillips and R. Milo: SARS-CoV-2 (COVID-19) by the numbers. *Elife*, 9 (2020) doi:10.7554/eLife.57309
4. J. Lan, J. Ge, J. Yu, S. Shan, H. Zhou, S. Fan, Q. Zhang, X. Shi, Q. Wang, L. Zhang and X. Wang: Structure of the SARS-CoV-2 spike receptor-binding domain bound to the ACE2 receptor. *Nature*, 581(7807), 215-220 (2020) doi:10.1038/s41586-020-2180-5
5. D. Wrapp, N. Wang, K. S. Corbett, J. A. Goldsmith, C. L. Hsieh, O. Abiona, B. S. Graham and J. S. McLellan: Cryo-EM structure of the 2019-nCoV spike in the prefusion conformation. *Science*, 367(6483), 1260-1263 (2020) doi:10.1126/science.abb2507
6. B. Korber, W. M. Fischer, S. Gnanakaran, H. Yoon, J. Theiler, W. Abfalterer, N. Hengartner, E. E. Giorgi, T. Bhattacharya, B. Foley, K. M. Hastie, M. D. Parker, D. G. Partridge, C. M. Evans, T. M. Freeman, T. I. de Silva, C.-G. G. Sheffield, C. McDanal, L. G. Perez, H. Tang, A. Moon-Walker, S. P. Whelan, C. C. LaBranche, E. O. Saphire and D. C. Montefiori: Tracking Changes in SARS-CoV-2 Spike: Evidence that D614G Increases Infectivity of the COVID-19 Virus. *Cell*, 182(4), 812-827 e19 (2020) doi:10.1016/j.cell.2020.06.043
7. A. Carrazco-Montalvo, A. Bruno, D. de Mora, M. Olmedo, J. Garces, M. Paez, M. Regato-Arrata, M. Gonzalez, J. Romero, O. Mestanza, B. Freire-Paspuel, A. Gaviria, S. A. Orlando, M. A. Garcia-Bereguiain and L. Patino: First Report of SARS-CoV-2 Lineage B.1.1.7 (Alpha Variant) in Ecuador, January 2021. *Infect Drug Resist*, 14, 5183-5188 (2021) doi:10.2147/IDR.S319439
8. S. Zarate, B. Taboada, J. E. Munoz-Medina, P. Isa, A. Sanchez-Flores, C. Boukadida, A. Herrera-Estrella, N. Selem Mojica, M. Rosales-Rivera, B. Gomez-Gil, A. G. Salas-Lais, C. E. Santacruz-Tinoco, H. Montoya-Fuentes, J. E. Alvarado-Yaah, G. M. Molina-Salinas, G. E. Espinoza-Ayala, J. A. Enciso-Moreno, R. M. Gutierrez-Rios, A. Loza, J. Moreno-Contreras, R. Garcia-Lopez, X. Rivera-Gutierrez, A. Comas-Garcia, R. M. Wong-Chew, M. E. Jimenez-Corona, R. M. Del Angel, J. A. Vazquez-Perez, M. Matias-Florentino, M. Perez-Garcia, S. Avila-Rios, H. G. Castelan-Sanchez, L. Delaye, L. P. Martinez-Castilla, M. Escalera-Zamudio, S. Lopez and C. F. Arias: The Alpha Variant (B.1.1.7) of SARS-CoV-2 Failed to Become Dominant in Mexico. *Microbiol Spectr*, 10(2), e0224021 (2022) doi:10.1128/spectrum.02240-21
9. H. Tegally, E. Wilkinson, M. Giovanetti, A. Iranzadeh, V. Fonseca, J. Giandhari, D. Doolabh, S. Pillay, E. J. San, N. Msomi, K. Mlisana, A. von Gottberg, S. Walaza, M. Allam, A. Ismail, T. Mohale, A. J. Glass, S. Engelbrecht, G. Van Zyl, W. Preiser, F. Petruccione, A. Sigal, D. Hardie, G. Marais, N.-y. Hsiao, S. Korsman, M.-A. Davies, L. Tyers, I. Mudau, D. York, C. Maslo, D. Goedhals, S. Abrahams, O. Laguda-Akingba, A. Alisoltani-Dehkordi, A. Godzik, C. K. Wibmer, B. T. Sewell, J. Lourenço, L. C. J. Alcantara, S. L. Kosakovsky Pond, S. Weaver, D. Martin, R. J. Lessells, J. N. Bhiman, C. Williamson and T. de Oliveira: Detection of a SARS-CoV-2 variant of concern in South Africa. *Nature*, 592(7854), 438-443 (2021) doi:10.1038/s41586-021-03402-9
10. T. Fujino, H. Nomoto, S. Kutsuna, M. Ujiie, T. Suzuki, R. Sato, T. Fujimoto, M. Kuroda, T. Wakita and N. Ohmagari: Novel SARS-CoV-2 Variant in Travelers from Brazil to Japan. *Emerg Infect Dis*, 27(4), 1243-5 (2021) doi:10.3201/eid2704.210138
11. M. Joshi, M. Kumar, V. Srivastava, D. Kumar, D. S. Rathore, R. Pandit, D. W. Graham and C. G. Joshi: Genetic sequencing detected the SARS-CoV-2 delta variant in wastewater a month prior to the first COVID-19 case in Ahmedabad (India). *Environ Pollut*, 310, 119757 (2022) doi:10.1016/j.envpol.2022.119757
12. K. Laiton-Donato, C. Franco-Munoz, D. A. Alvarez-Diaz, H. A. Ruiz-Moreno, J. A. Usme-Ciro, D. A. Prada, J. Reales-Gonzalez, S. Corchuelo, M. T. Herrera-Sepulveda, J. Naizaque, G. Santamaria, J. Rivera, P. Rojas, J. H. Ortiz, A. Cardona, D. Malo, F. Prieto-Alvarado, F. R. Gomez, M. Wiesner, M. L. O. Martinez and M. Mercado-Reyes: Characterization of the emerging B.1.621 variant of interest of SARS-CoV-2. *Infect Genet Evol*, 95, 105038 (2021) doi:10.1016/j.meegid.2021.105038

13. P. L. Wink, F. C. Z. Volpato, F. L. Monteiro, J. B. Willig, A. P. Zavascki, A. L. Barth and A. F. Martins: First identification of SARS-CoV-2 lambda (C.37) variant in Southern Brazil. *Infect Control Hosp Epidemiol*, 43(12), 1996-1997 (2022) doi:10.1017/ice.2021.390
14. COVID-19 Weekly Epidemiological Update Edition 44, published 15 June 2021. *World Health Organization* (2021)
15. J. Quarleri, V. Galvan and M. V. Delpino: Omicron variant of the SARS-CoV-2: a quest to define the consequences of its high mutational load. *Geroscience*, 44(1), 53-56 (2022) doi:10.1007/s11357-021-00500-4
16. A. Gowrisankar, T. M. C. Priyanka and S. Banerjee: Omicron: a mysterious variant of concern. *Eur Phys J Plus*, 137(1), 100 (2022) doi:10.1140/epjp/s13360-021-02321-y
17. A. Vitiello, F. Ferrara, A. M. Auti, M. Di Domenico and M. Boccellino: Advances in the Omicron variant development. *J Intern Med*, 292(1), 81-90 (2022) doi:10.1111/joim.13478
18. Y. Fan, X. Li, L. Zhang, S. Wan, L. Zhang and F. Zhou: SARS-CoV-2 Omicron variant: recent progress and future perspectives. *Signal Transduct Target Ther*, 7(1), 141 (2022) doi:10.1038/s41392-022-00997-x
19. J. Fonager, M. Bennedbaek, P. Bager, J. Wohlfahrt, K. M. Ellegaard, A. C. Ingham, S. M. Edslev, M. Stegger, R. N. Sieber, R. Lassauniere, A. Fomsgaard, T. Lillebaek, C. W. Svarrer, F. T. Moller, C. H. Moller, R. Legarth, T. V. Sydenham, K. Steinke, S. J. Paulsen, J. A. S. Castruita, U. V. Schneider, C. H. Schouw, X. C. Nielsen, M. Overvad, R. T. Nielsen, R. L. Marvig, M. S. Pedersen, L. Nielsen, L. L. Nilsson, J. Bybjerg-Grauholm, I. H. Tarpgaard, T. S. Ebsen, J. U. H. Lam, V. Gunalan and M. Rasmussen: Molecular epidemiology of the SARS-CoV-2 variant Omicron BA.2 sub-lineage in Denmark, 29 November 2021 to 2 January 2022. *Euro Surveill*, 27(10) (2022) doi:10.2807/1560-7917.ES.2022.27.10.2200181
20. L. B. Shrestha, C. Foster, W. Rawlinson, N. Tedla and R. A. Bull: Evolution of the SARS-CoV-2 omicron variants BA.1 to BA.5: Implications for immune escape and transmission. *Rev Med Virol*, 32(5), e2381 (2022) doi:10.1002/rmv.2381
21. L. Yao, K. L. Zhu, X. L. Jiang, X. J. Wang, B. D. Zhan, H. X. Gao, X. Y. Geng, L. J. Duan, E. H. Dai and M. J. Ma: Omicron subvariants escape antibodies elicited by vaccination and BA.2.2 infection. *Lancet Infect Dis*, 22(8), 1116-1117 (2022) doi:10.1016/S1473-3099(22)00410-8
22. S. Torii, C. Ono, R. Suzuki, Y. Morioka, I. Anzai, Y. Fauzyah, Y. Maeda, W. Kamitani, T. Fukuhara and Y. Matsuura: Establishment of a reverse genetics system for SARS-CoV-2 using circular polymerase extension reaction. *Cell Rep*, 35(3), 109014 (2021) doi:10.1016/j.celrep.2021.109014
23. T. Y. Taha, I. P. Chen, J. M. Hayashi, T. Tabata, K. Walcott, G. R. Kimmerly, A. M. Syed, A. Ciling, R. K. Suryawanshi, H. S. Martin, B. H. Bach, C. L. Tsou, M. Montano, M. M. Khalid, B. K. Sreekumar, G. Renuka Kumar, S. Wyman, J. A. Doudna and M. Ott: Rapid assembly of SARS-CoV-2 genomes reveals attenuation of the Omicron BA.1 variant through NSP6. *Nat Commun*, 14(1), 2308 (2023) doi:10.1038/s41467-023-37787-0
24. W. Wang, X. Peng, Y. Jin, J. A. Pan and D. Guo: Reverse genetics systems for SARS-CoV-2. *J Med Virol*, 94(7), 3017-3031 (2022) doi:10.1002/jmv.27738
25. L. Xu, L. Bao, Q. Lv, W. Deng, Y. Ma, F. Li, L. Zhan, H. Zhu, C. Ma and C. Qin: A single-amino-acid substitution in the HA protein changes the replication and pathogenicity of the 2009 pandemic A (H1N1) influenza viruses in vitro and in vivo. *Virol J*, 7, 325 (2010) doi:10.1186/1743-422X-7-325
26. L. A. Silva, S. Khomandiak, A. W. Ashbrook, R. Weller, M. T. Heise, T. E. Morrison and T. S. Dermody: A single-amino-acid polymorphism in Chikungunya virus E2 glycoprotein influences glycosaminoglycan utilization. *J Virol*, 88(5), 2385-97 (2014) doi:10.1128/JVI.03116-13
27. K. A. Tsetsarkin, D. L. Vanlandingham, C. E. McGee and S. Higgs: A single mutation in chikungunya virus affects vector specificity and epidemic potential. *PLoS Pathog*, 3(12), e201 (2007) doi:10.1371/journal.ppat.0030201
28. X. C. Tang, S. S. Agnihothram, Y. Jiao, J. Stanhope, R. L. Graham, E. C. Peterson, Y. Avnir, A. S. Tallarico, J. Sheehan, Q. Zhu, R. S. Baric and W. A. Marasco: Identification of human neutralizing antibodies against MERS-CoV and their role in virus adaptive evolution. *Proc Natl Acad Sci U S A*, 111(19), E2018-26 (2014) doi:10.1073/pnas.1402074111
29. J. Sui, D. R. Aird, A. Tamin, A. Murakami, M. Yan, A. Yammanuru, H. Jing, B. Kan, X. Liu, Q. Zhu, Q. A. Yuan, G. P. Adams, W. J. Bellini, J. Xu, L. J. Anderson and W. A. Marasco: Broadening of neutralization activity to directly block a dominant antibody-driven SARS-coronavirus evolution pathway. *PLoS Pathog*, 4(11), e1000197 (2008) doi:10.1371/journal.ppat.1000197

30. J. ter Meulen, E. N. van den Brink, L. L. Poon, W. E. Marissen, C. S. Leung, F. Cox, C. Y. Cheung, A. Q. Bakker, J. A. Bogaards, E. van Deventer, W. Preiser, H. W. Doerr, V. T. Chow, J. de Kruif, J. S. Peiris and J. Goudsmit: Human monoclonal antibody combination against SARS coronavirus: synergy and coverage of escape mutants. *PLoS Med*, 3(7), e237 (2006) doi:10.1371/journal.pmed.0030237
31. L. van Dorp, D. Richard, C. C. S. Tan, L. P. Shaw, M. Acman and F. Balloux: No evidence for increased transmissibility from recurrent mutations in SARS-CoV-2. *Nat Commun*, 11(1), 5986 (2020) doi:10.1038/s41467-020-19818-2

Conflict of Interest

The authors declare that the research was conducted in the absence of any commercial or financial relationships that could be construed as a potential conflict of interest.

Figure legends

Fig. 1. Mutation subsets of S protein of SARS-CoV-2 variants.

Sequences of S protein of SARS-CoV-2 variants（variants of concern, VOCs: Alpha:B.1.1.7, Beta:B.1.351, Gamma:P1, Delta:B.1.617.2.63, and Omicron:BA.1; BA.2 and variants of interest, VOIs: Lambda:C.37, Mu:B.1.621) are compared with the SARS-CoV-2 Wuhan-Hu-H1 reference sequence, and different amino acids (amino acid change, deletion, and insertion) and synonymous changes of nucleotides are shown. Non-synonymous changes are shown by amino acid changes (capital letters), and synonymous changes are shown by nucleotide changes (small letters). Amino acids different from Wuhan-Hu-H1 found in each variant: Alpha: B.1.1.7, Beta: B.1.351, Gamma: P1, Delta: B.1.617.2.63, Lambda: C.37, Mu: B.1.621, and Omicron: BA.1, BA.2 are highlighted with red, orange, green, yellow, aquamarine, lime, deep sky blue, and blue violet, respectively. Amino acid changes common to Omicron: BA.1 and BA.2 are shown in purple.

Fig. 2. Mutations of S proteins of SARS-CoV-2 Omicron isolates.

(A) Different amino acids and synonymous changes of nucleotides in **S** proteins of SARS-CoV-2 Omicron BA.1, BA.1.1 isolates, and BA.1-0.1s compared with SARS-CoV-2 Wuhan-Hu-H1. Nucleotide deletions and insertions were "deletion^{1}" (deletion: nt 21,766-21,771), "deletion^{2}" (deletion: nt 21,987-21,995), "deletion^{3}" (deletion: nt 22,194-22,196), and "insertion^{4}" (insertion between 22,206-22,196), and introduced amino acid changes were H69-_V70-, G142D_V143-_Y144-_Y145-, N211I_L212-, and 215ins.EPE, respectively. (B) Different amino acids and synonymous nucleotide changes in S proteins of SARS-CoV-2 Omicron BA.1.1-0.1 isolates. Amino acids different from Wuhan-Hu-H1 found in each variant: Alpha: B.1.1.7, Beta: B.1.351, Gamma: P1, Delta: B.1.617.2.63, Mu: B.1.621, and Omicron: BA.1, BA.2 are highlighted with red, orange, green, yellow, lime, deep sky blue, and blue violet, respectively. Amino acid changes common to Omicron:BA.1 and BA.2 are highlighted with purple.

Fig. 3. Estimated homologous recombination breakpoints of the SARS-CoV-2 S gene of Omicron BA.1-0.1 or BA.1.1-0.1.

Sequence alignment of amino acids and their coding nucleotides (nt.21,746-21,787; nt.22,658-22,702; nt.22,976-23,011, and nt.23,582-23,620) containing the mutation point of the SARS-CoV-2 S gene of the Omicron BA.1 variant compared with SARS-CoV-2 Wuhan-Hu-H1. Changed nucleotides and amino acids of Omicron BA.1 are shown in red letters. Estimated homologous recombination breakpoints of the SARS-CoV-2 S gene of Omicron BA.1-0.1 or BA.1.1-0.1 are shown by asterisks.

Fig. 4. Representative mutations of SARS-CoV-2 Omicron isolates other than S protein.

(A) Representative amino acids and synonymous changes of nucleotides of SARS-CoV-2 Omicron BA.1, BA.1.1 isolates, and BA.1-0.1 compared with SARS-CoV-2 Wuhan-Hu-H1. **(B)** Representative amino acids and synonymous changes of nucleotides of SARS-CoV-2 Omicron BA.1.1-0.1 compared with SARS-CoV-2 Wuhan-Hu-H1. Amino acids different from Wuhan-Hu-H1 found in each variant: Alpha: B.1.1.7, Lambda: C.37, Mu: B.1.621, and Omicron: BA.1 are highlighted with red, aquamarine, deep sky blue, and blue violet, respectively.

Amino acid changes common to Omicron: BA.1 and BA.2 are shown in purple. Synonymous nucleotide changes: c2470u observed in Omicron:BA.1.1 mainly shown with blue. Synonymous and non-synonymous changes: u10135c of nsp5, L106F in ORF3, and D343G in N protein subset observed in ~40% of Omicron;

BA.1-0.1 are highlighted with emerald-green. Undetermined nucleotides or amino acids are shown as UD or X, respectively.

Fig. 5. Mutations of S proteins of SARS-CoV-2 Omicron BA.1-BA.2 recombinant isolates and SARS-CoV-2 Omicron BA.1 and BA.2 isolates detected in Puerto Rico in 2020.

(A) Different amino acids and synonymous change of nucleotides in S proteins of SARS-CoV-2 Omicron BA.1-BA.2 recombinant isolates compared with SARS-CoV-2 Wuhan-Hu-H1. Nucleotide deletions, "deletion^{5}" (deletion: nt 21,633-21,641), introduced the amino acids changes L24-_P25-_P26-_A27S. **(B)** Different amino acids and synonymous change of nucleotides in S proteins of SARS-CoV-2 Omicron BA.1.1 and Omicron BA.1-BA.2 recombinant isolate, highlighted with magenta (GenBank: ON928946.1), Omicron BA.2, and Omicron 2-0.1(K440N), detected in Puerto Rico in 2020. Amino acids different from Wuhan-Hu-H1 found in each variant: Alpha: B.1.1.7, Beta: B.1.351, Gamma: P1, Delta: B.1.617.2.63, Mu: B.1.621, and Omicron: BA.1, BA.2 are highlighted with red, orange, green, yellow, lime, deep sky blue, and blue-violet, respectively. Amino acid changes common to Omicron: BA.1 and BA.2 are highlighted with purple.

Supplemental Figure 1

Human coronavirus 229E strains detected in Seattle, USA, in 2015 and 2019.

Alignment of nucleotide **(A)** and amino acid **(B)** sequences of the S protein of Human coronavirus 229E strains, HCoV_229E/Seattle/USA/SC3112/2015 (GenBank: KY983587.1), and CoV_229E/Seattle/USA/SC0865/2019 (GenBank: MN306046.1). The number of nucleotide substitutions observed between them was 32, amino acid substitutions numbered 18 between them, and the synonymous (14: 32-18)–non-synonymous mutation (18) rate between them was 1.285

Supplemental Figure 2

Different amino acids and synonymous changes of nucleotides in S proteins of SARS-CoV-2 Omicron BA.2 isolates and BA.2-0.1s compared with SARS-CoV-2 Wuhan-Hu-H1.

Nucleotide deletions, "deletion^{5}" (deletion: nt 21,633-21,641), introduced the amino acid changes L24-_P25-_P26-_A27S. Amino acids different from Wuhan-Hu-H1 found in each variant: Alpha: B.1.1.7, Beta: B.1.351, Gamma: P1, Delta: B.1.617.2.63, Mu: B.1.621, and Omicron: BA.1, BA.2 are highlighted with red, orange, green, yellow, lime, deep sky blue, and blue-violet, respectively. Amino acid changes common to Omicron: BA.1 and BA.2 are highlighted with purple.

Supplemental Figure 3

Estimated homologous recombination breakpoints of the SARS-CoV-2 S gene of the Omicron BA.2-0.1 or BA.1-BA.2 recombinant.

(A) Sequence alignment of the amino acids and coding nucleotides (nt. 22,658-22,702) containing the mutation point of the SARS-CoV-2 S gene of Omicron BA.2 variants compared with SARS-CoV-2 Wuhan-Hu-H1. **(B)** Sequence alignment of the amino acids and coding nucleotides (nt. 22,178-22,222) containing the mutation point of the SARS-CoV-2 S gene of Omicron BA,1, BA.2 variant and BA.1-BA.2 recombinant isolate compared with SARS-CoV-2 Wuhan-Hu-H1. Changed nucleotides and amino acids of Omicron variants BA.1, BA.2, and

615 BA.1-BA.2 recombinant isolates compared with SARS-CoV-2 Wuhan-Hu-H1 sequences are shown in red
616 letters. Asterisks show an estimated homologous recombination breakpoint of the SARS-CoV-2 S gene of
617 Omicron BA.2-0.1.

Fig. 1

Variant	Definition	Accession No.	Non-synonymous: S1
	SARS-CoV-2_Wuhan-Hu-1	GenBank: NC_045512.2	
20I (Alpha, V1) B.1.1.7	SARS-CoV-2_human_ITA_CL106_2020	GenBank: MW423686.2	H69-, V70-, Y144-
	SARS-CoV-2_human_USA_CA-CDC-STM-P017_2020	GenBank: MW430966.1	H69-, V70-, Y144-
	SARS-CoV-2_human_USA_CA-CDC-STM-P019_2020	GenBank: MW430967.1	H69-, V70-, Y144-
	SARS-CoV-2_human_USA_CO-CDPHE-2100156850_2020	GenBank: MW422256.1	H69-, V70-, Y144-
20H (Beta, V2) B.1.351	SARS-CoV-2_human_GHA_nmimr-SARS-CoV-2-TRA-201_2021	GenBank: MW598419.1	D80A, D215G, L241-, L242-, A243-
	SARS-CoV-2_human_USA_SC-CDC-LC0010408_2021	GenBank: MW667552.1	D80A, D215G, L241-, L242-, A243-
	SARS-CoV-2_human_USA_NC-CDC-LC0010422_2021	GenBank: MW667553.1	D80A, D215G, L241-, L242-, A243-
	SARS-CoV-2_human_USA_MD-CDC-LC0015967_2021	GenBank: MW721502.1	D80A, D215G, L241-, L242-, A243-
	SARS-CoV-2_human_USA_NC-CDC-LC0016056_2021	GenBank: MW721504.1	D80A, D215G, L241-, L242-, A243-
20J (Gamma, V3) P.1 and	SARS-CoV-2_human_USA_MN-MDH-2399_2021	GenBank: MW520923.1	L18F, T20N, P26S, D138Y, R190S
	SARS-CoV-2_human_ITA_ABR-IZSGC-TE30939_2021	GenBank: MW642248.1	L18F, T20N, P26S, D138Y, R190S
	SARS-CoV-2_human_ITA_ABR-IZSGC-TE30964_2021	GenBank: MW642249.1	L18F, T20N, P26S, D138Y, R190S
	SARS-CoV-2_human_ITA_ABR-IZSGC-TE30968_2021	GenBank: MW642250.1	L18F, T20N, P26S, D138Y, R190S
21I (Delta). B.1.617.2.63	SARS-CoV-2_human_USA_CA-CDC-LC0056316_2021	GenBank: MZ182066.1	T19R, G142D, E156-, F157-, R158G, A222V
	SARS-CoV-2_human_USA_FL-CDC-FG-029410_2021	GenBank: MZ155303.1	T19R, G142D, E156-, F157-, R158G, A222V
	SARS-CoV-2_human_USA_FL-CDC-FG-029674_2021	GenBank: MZ155230.1	T19R, G142D, E156-, F157-, R158G, A222V
	SARS-CoV-2_human_USA_MA-MASPHL-03599_2021	GenBank: MZ170364.1	T19R, G142D, E156-, F157-, R158G, A222V
	SARS-CoV-2_human_USA_NJ-CDC-LC0054029_2021	GenBank: MZ179869.1	T19R, G142D, E156-, F157-, R158G, A222V
21G (Lambda) C.37	SARS-CoV-2_human_USA_FL-CDC-QDX21609207_2021	GenBank: MW666666.1	G75V, T76I, R246-, S247-, Y248-, L249-, T250-, P251-, G252-, D253N
	SARS-CoV-2_human_USA_FL-CDC-QDX22062355_2021	GenBank: MW696612.1	G75V, T76I, R246-, S247-, Y248-, L249-, T250-, P251-, G252-, D253N
	SARS-CoV-2_human_USA_FL-CDC-QDX22120927_2021	GenBank: MW699217.1	G75V, T76I, R246-, S247-, Y248-, L249-, T250-, P251-, G252-, D253N
	SARS-CoV-2_human_USA_MD-MDH-0957_2021	GenBank: MW644498.1	G75V, T76I, R246-, S247-, Y248-, L249-, T250-, P251-, G252-, D253N
21H (Mu) B.1.621	SARS-CoV-2_human_USA_FL-CDC-2-4653360_2021	GenBank: MZ727706.1	T95I, Y144S, Y145N
	SARS-CoV-2_human_USA_JW1506_2021	GenBank: MZ620161.1	T95I, Y144S, Y145N
	SARS-CoV-2_human_USA_LA-BIE-LSUH001268_2021	GenBank: MZ637380.1	T95I, Y144S, Y145N
	SARS-CoV-2_human_USA_LA-BIE-LSUH001328_2021	GenBank: MZ637401.1	T95I, Y144S, Y145N
	SARS-CoV-2_human_USA_RI-CDC-2-4462325_2021	GenBank: MZ780550.1	T95I, Y144S, Y145N
BA.1 (Omicron)	SARS-CoV-2_human_BEL_rega-20174_2021	GenBank: OL672836.1	A67V, H69-, V70-, T95I, G142D, V143-, Y144-, Y145-, N211-, L212I, 215ins. EPE
	SARS-CoV-2_human_CAN_ON-NML-249359_2021	GenBank: OL677199.1	A67V, H69-, V70-, T95I, G142D, V143-, Y144-, Y145-, N211-, L212I, 215ins. EPE
	SARS-CoV-2_human_USA_CA-CDPH-7000007788_2022	GenBank: OP769083.1	A67V, H69-, V70-, T95I, G142D, V143-, Y144-, Y145-, N211-, L212I, 215ins. EPE
	SARS-CoV-2_human_USA_FL-BPHL-16914_2021	GenBank: OL764360.1	A67V, H69-, V70-, T95I, G142D, V143-, Y144-, Y145-, N211-, L212I, 215ins. EPE
	SARS-CoV-2_human_USA_GA-CDC-STM-YNPP52544_2021	GenBank: OL815447.1	A67V, H69-, V70-, T95I, G142D, V143-, Y144-, Y145-, N211-, L212I, 215ins. EPE
	SARS-CoV-2_human_USA_TX-HHD-2205174858_2021	GenBank: ON762438.1	A67V, H69-, V70-, T95I, G142D, V143-, Y144-, Y145-, N211-, L212I, 215ins. EPE
BA.2 (Omicron)	SARS-CoV-2_human_USA_CA-CDC-FG-229617_2021	GenBank: OM233931.1	T19I, L24-, P25-, P26-, A27S, G142D, V213G
	SARS-CoV-2_human_USA_MA-CDCBI-CRSP_AJSZPA3XZ6CDKXX5_2021	GenBank: OM072551.1	T19I, L24-, P25-, P26-, A27S, G142D, V213G
	SARS-CoV-2_human_USA_MA-CDCBI-CRSP_URIKNCKBF5674VF4_2021	GenBank: OM072822.1	T19I, L24-, P25-, P26-, A27S, G142D, V213G
	SARS-CoV-2_human_USA_WA-S16116_2022	GenBank: OM296922.1	T19I, L24-, P25-, P26-, A27S, G142D, V213G

Variant	Definition	Non-synonymous: S1 – Receptor-binding domain (RBD) 319 – 541	Non-synonymous: S1	Non-synonymous: S2	Synonymous
	SARS-CoV-2_Wuhan-Hu-1				
20I (Alpha, V1) B.1.1.7	SARS-CoV-2_human_ITA_CL106_2020	N501Y	A570D, D614G, P681H	T716I, S982A, D1118H	
	SARS-CoV-2_human_USA_CA-CDC-STM-P017_2020	N501Y	A570D, D614G, P681H	T716I, S982A, D1118H	
	SARS-CoV-2_human_USA_CA-CDC-STM-P019_2020	N501Y	A570D, D614G, P681H	T716I, S982A, D1118H	
	SARS-CoV-2_human_USA_CO-CDPHE-2100156850_2020	N501Y	A570D, D614G, P681H	T716I, S982A, D1118H	
20H (Beta, V2) B.1.351	SARS-CoV-2_human_GHA_nmimr-SARS-CoV-2-TRA-201_2021	K417N, E484K, N501Y	D614G	A701V	
	SARS-CoV-2_human_USA_SC-CDC-LC0010408_2021	K417N, E484K, N501Y	D614G	A701V	
	SARS-CoV-2_human_USA_NC-CDC-LC0010422_2021	K417N, E484K, N501Y	D614G	A701V	
	SARS-CoV-2_human_USA_MD-CDC-LC0015967_2021	K417N, E484K, N501Y	D614G	A701V	
	SARS-CoV-2_human_USA_NC-CDC-LC0016056_2021	K417N, E484K, N501Y	D614G	A701V	
20J (Gamma, V3) P.1 and	SARS-CoV-2_human_USA_MN-MDH-2399_2021	K417T, E484K, N501Y	D614G, H655Y	T1027I, V1176F	c23380u
	SARS-CoV-2_human_ITA_ABR-IZSGC-TE30939_2021	K417T, E484K, N501Y	D614G, H655Y	T1027I, V1176F	
	SARS-CoV-2_human_ITA_ABR-IZSGC-TE30964_2021	K417T, E484K, N501Y	D614G, H655Y	T1027I, V1176F	
	SARS-CoV-2_human_ITA_ABR-IZSGC-TE30968_2021	K417T, E484K, N501Y	D614G, H655Y	T1027I, V1176F	
21I (Delta). B.1.617.2.63	SARS-CoV-2_human_USA_CA-CDC-LC0056316_2021	L452R, T478K	D614G, P681R	D950N	
	SARS-CoV-2_human_USA_FL-CDC-FG-029410_2021	L452R, T478K	D614G, P681R	D950N	c21622u
	SARS-CoV-2_human_USA_FL-CDC-FG-029674_2021	L452R, T478K	D614G, P681R	D950N	c21622u
	SARS-CoV-2_human_USA_MA-MASPHL-03599_2021	L452R, T478K	D614G, P681R	D950N	
	SARS-CoV-2_human_USA_NJ-CDC-LC0054029_2021	L452R, T478K	D614G, P681R	D950N	
21G (Lambda) C.37	SARS-CoV-2_human_USA_FL-CDC-QDX21609207_2021	L452Q, F490S	D614G	T859N	c23731u
	SARS-CoV-2_human_USA_FL-CDC-QDX22062355_2021	L452Q, F490S	D614G	T859N	c23731u
	SARS-CoV-2_human_USA_FL-CDC-QDX22120927_2021	L452Q, F490S	D614G	T859N	c23731u
	SARS-CoV-2_human_USA_MD-MDH-0957_2021	L452Q, F490S	D614G	T859N	c23731u
21H (Mu) B.1.621	SARS-CoV-2_human_USA_FL-CDC-2-4653360_2021	R346K, E484K, N501Y	D614G, P681H	D950N	
	SARS-CoV-2_human_USA_JW1506_2021	R346K, E484K, N501Y	D614G, P681H	D950N	
	SARS-CoV-2_human_USA_LA-BIE-LSUH001268_2021	R346K, E484K, N501Y	D614G, P681H	D950N	t22384a
	SARS-CoV-2_human_USA_LA-BIE-LSUH001328_2021	R346K, E484K, N501Y	D614G, P681H	D950N	t22384a
	SARS-CoV-2_human_USA_RI-CDC-2-4462325_2021	R346K, E484K, N501Y	D614G, P681H	D950N	t22384a
BA.1 (Omicron)	SARS-CoV-2_human_BEL_rega-20174_2021	G339D, S371L, S373P, S375F, K417N, N440K, G446S, S477N, T478K, E484A, Q493R, G496S, Q498R, N501Y, Y505H	T547K, D614G, H655Y, N679K, P681H	N764K, D796Y, N856K, Q954H, N969K, L981F	c25000u
	SARS-CoV-2_human_CAN_ON-NML-249359_2021	G339D, S371L, S373P, S375F, K417N, N440K, G446S, S477N, T478K, E484A, Q493R, G496S, Q498R, N501Y, Y505H	T547K, D614G, H655Y, N679K, P681H	N764K, D796Y, N856K, Q954H, N969K, L981F	c25000u
	SARS-CoV-2_human_USA_CA-CDPH-7000007788_2022	G339D, S371L, S373P, S375F, K417N, N440K, G446S, S477N, T478K, E484A, Q493R, G496S, Q498R, N501Y, Y505H	T547K, D614G, H655Y, N679K, P681H	N764K, D796Y, N856K, Q954H, N969K, L981F	c25000u
	SARS-CoV-2_human_USA_FL-BPHL-16914_2021	G339D, S371L, S373P, S375F, K417N, N440K, G446S, S477N, T478K, E484A, Q493R, G496S, Q498R, N501Y, Y505H	T547K, D614G, H655Y, N679K, P681H	N764K, D796Y, N856K, Q954H, N969K, L981F	c25000u
	SARS-CoV-2_human_USA_GA-CDC-STM-YNPP52544_2021	G339D, S371L, S373P, S375F, K417N, N440K, G446S, S477N, T478K, E484A, Q493R, G496S, Q498R, N501Y, Y505H	T547K, D614G, H655Y, N679K, P681H	N764K, D796Y, N856K, Q954H, N969K, L981F	c25000u
	SARS-CoV-2_human_USA_TX-HHD-2205174858_2021	G339D, S371L, S373P, S375F, K417N, N440K, G446S, S477N, T478K, E484A, Q493R, G496S, Q498R, N501Y, Y505H	T547K, D614G, H655Y, N679K, P681H	N764K, D796Y, N856K, Q954H, N969K, L981F	c25000u
BA.2 (Omicron)	SARS-CoV-2_human_USA_CA-CDC-FG-229617_2021	G339D, S371F, S373P, S375F, T376A, D405N, R408S, K417N, N440K, S477N, T478K, E484A, Q493R, Q498R, N501Y, Y505H	D614G, H655Y, N679K, P681H	N764K, D796Y, Q954H, N969K	c25000u
	SARS-CoV-2_human_USA_MA-CDCBI-CRSP_AJSZPA3XZ6CDKXX5_2021	G339D, S371F, S373P, S375F, T376A, D405N, R408S, K417N, N440K, S477N, T478K, E484A, Q493R, Q498R, N501Y, Y505H	D614G, H655Y, N679K, P681H	N764K, D796Y, Q954H, N969K	c22792u, c25000u
	SARS-CoV-2_human_USA_MA-CDCBI-CRSP_URIKNCKBF5674VF4_2021	G339D, S371F, S373P, S375F, T376A, D405N, R408S, K417N, N440K, S477N, T478K, E484A, Q493R, Q498R, N501Y, Y505H	D614G, H655Y, N679K, P681H	N764K, D796Y, Q954H, N969K	c22792u, c25000u
	SARS-CoV-2_human_USA_WA-S16116_2022	G339D, S371F, S373P, S375F, T376A, D405N, R408S, K417N, N440K, S477N, T478K, E484A, Q493R, Q498R, N501Y, Y505H	D614G, H655Y, N679K, P681H	N764K, D796Y, Q954H, N969K	c25000u

Fig. 2 A

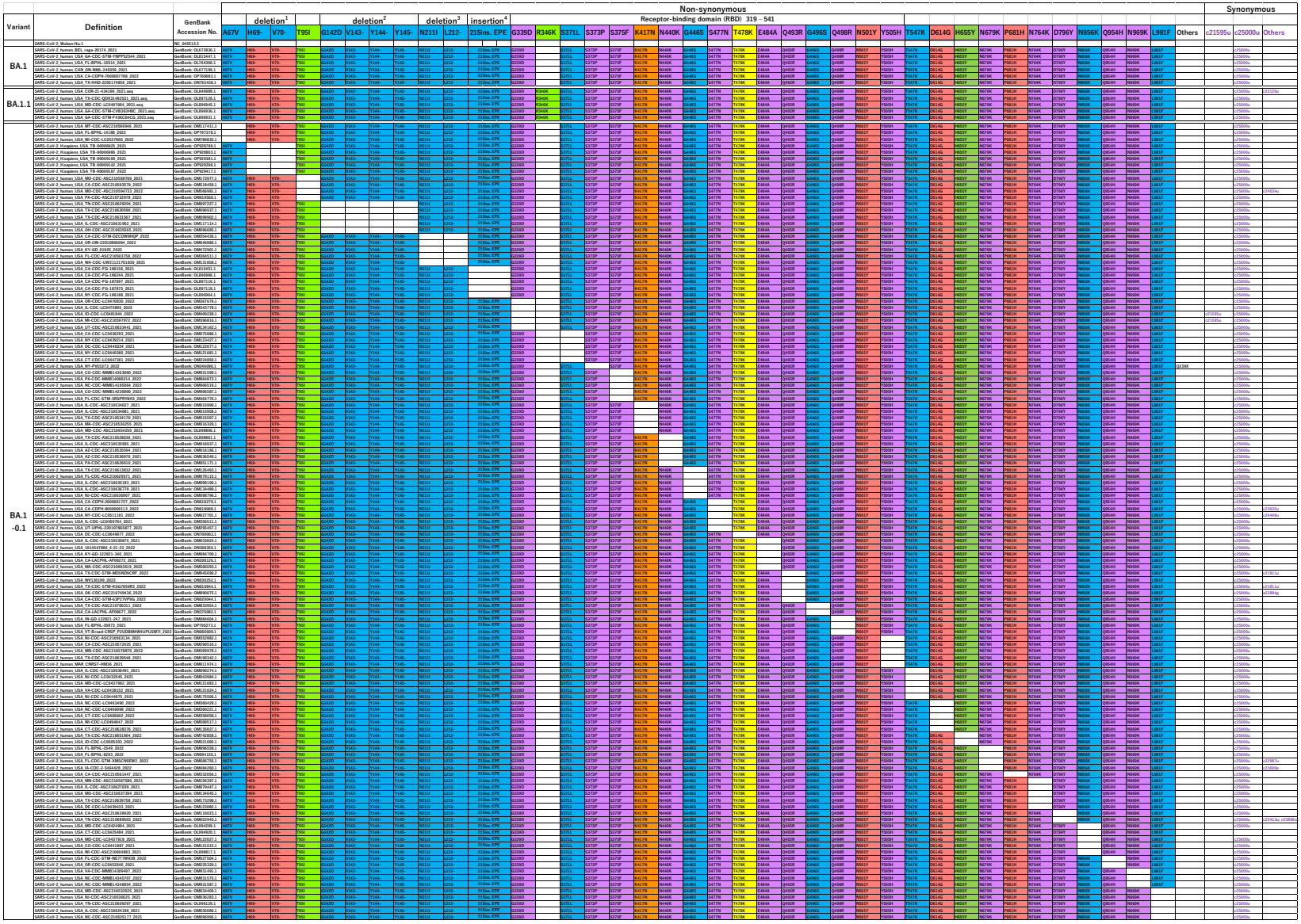

Fig. 2 B

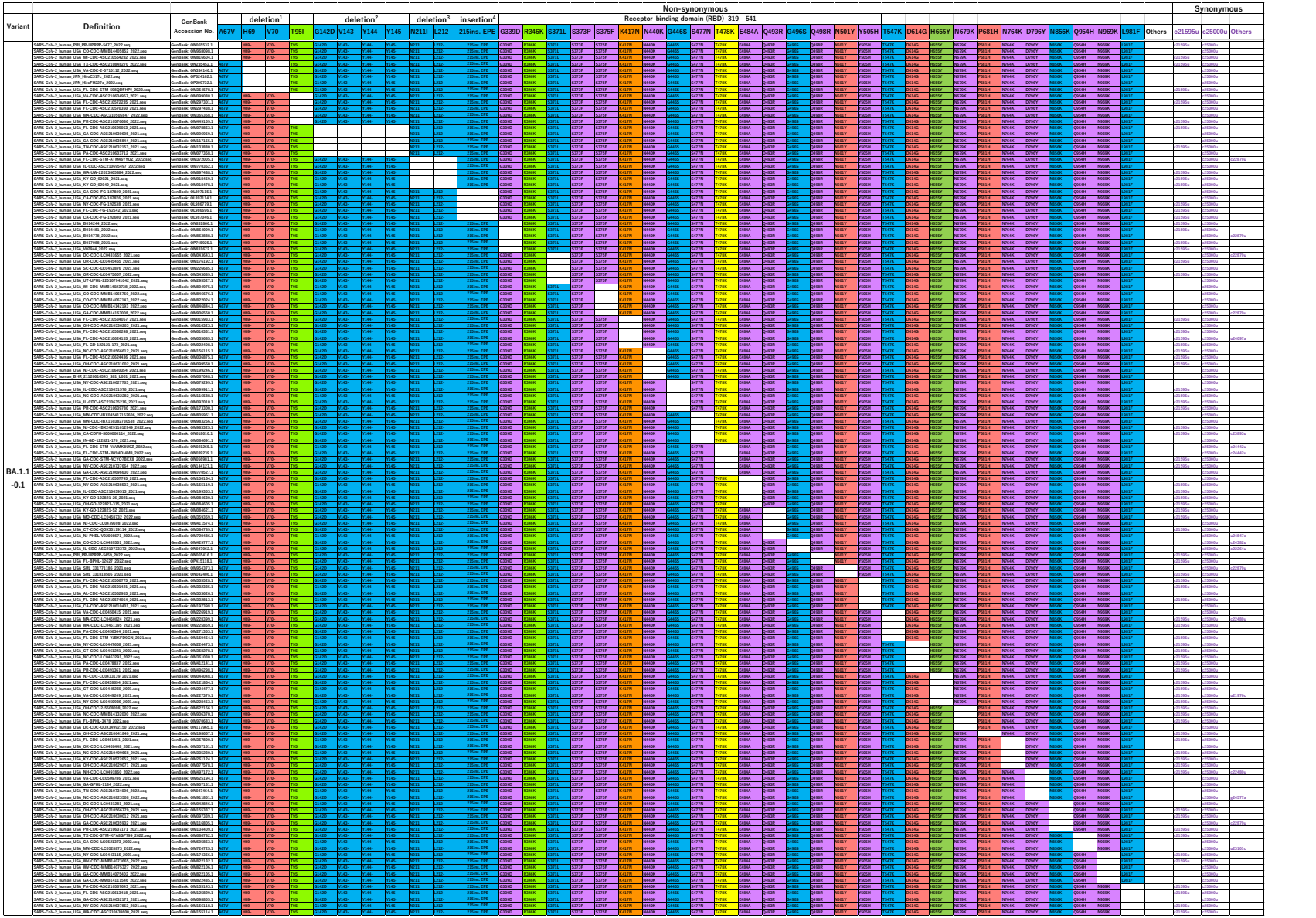

Fig. 3

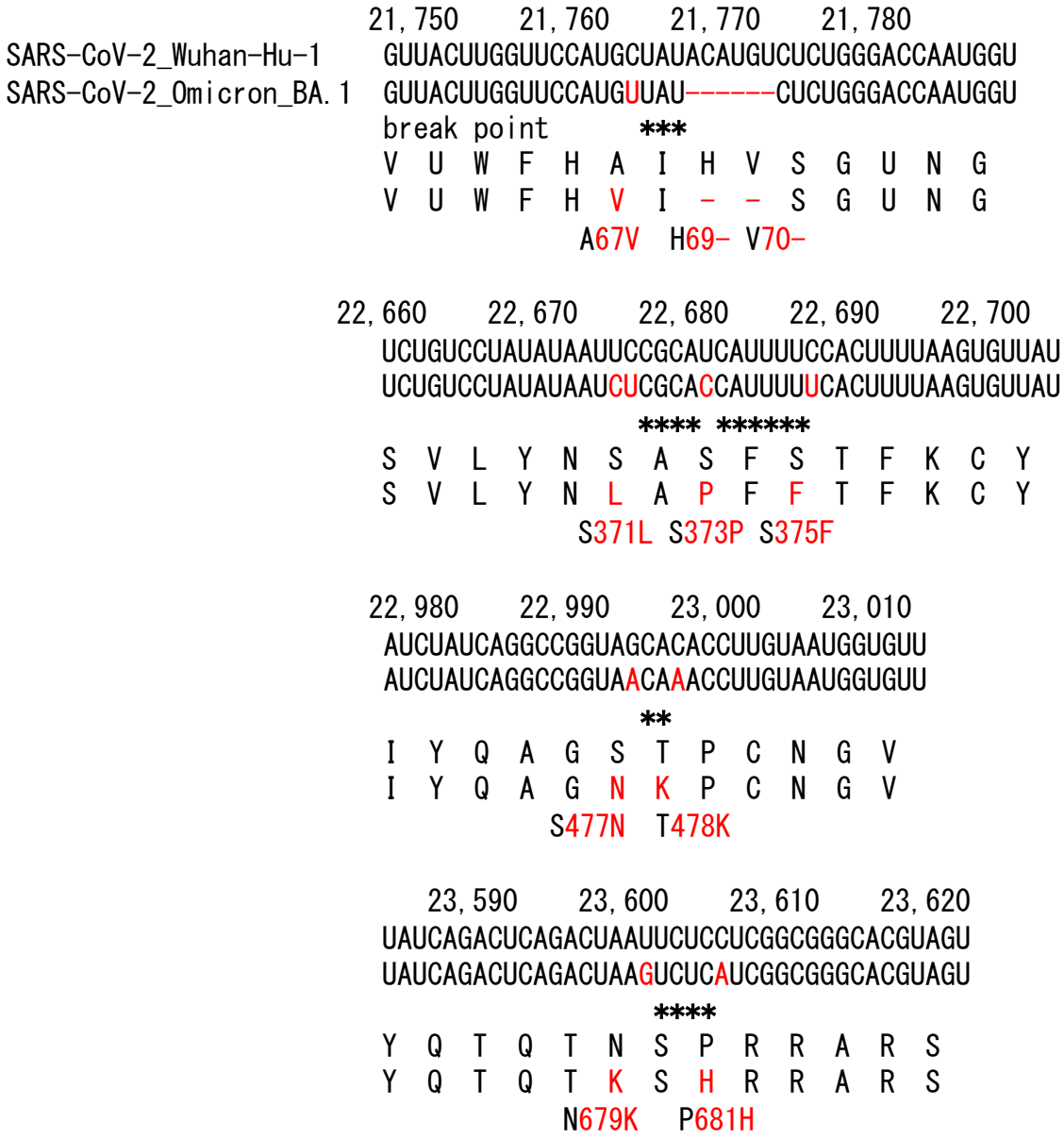
21,750 21,760 21,770 21,780
SARS-CoV-2_Wuhan-Hu-1 GUUACUUGGUUCCAUGCUAUACAUGUCUCUGGGACCAAUGGU
SARS-CoV-2_Omicron_BA.1 GUUACUUGGUUCCAUGUUAU------CUCUGGGACCAAUGGU
break point ***
V U W F H A I H V S G U N G
V U W F H V I - - S G U N G
A67V H69- V70-
22,660 22,670 22,680 22,690 22,700
UCUGUCCUAUAUAAUUCCGCAUCAUUUUCCACUUUUAAGUGUUAU
UCUGUCCUAUAUAAUCUCGCACCAUUUUUCACUUUUAAGUGUUAU
**** ******
S V L Y N S A S F S T F K C Y
S V L Y N L A P F F T F K C Y
S371L S373P S375F
22,980 22,990 23,000 23,010
AUCUAUCAGGCCGGUAGCACACCUUGUAAUGGUGUU
AUCUAUCAGGCCGGUAACAACCUUGUAAUGGUGUU
**
I Y Q A G S T P C N G V
I Y Q A G N K P C N G V
S477N T478K
23,590 23,600 23,610 23,620
UAUCAGACUCAGACUAAUUCUCCUCGGCGGGCACGUAGU
UAUCAGACUCAGACUAAGUCUCAUCGGCGGGCACGUAGU
****
Y Q T Q T N S P R R A R S
Y Q T Q T K S H R R A R S
N679K P681H

Fig. 4 A

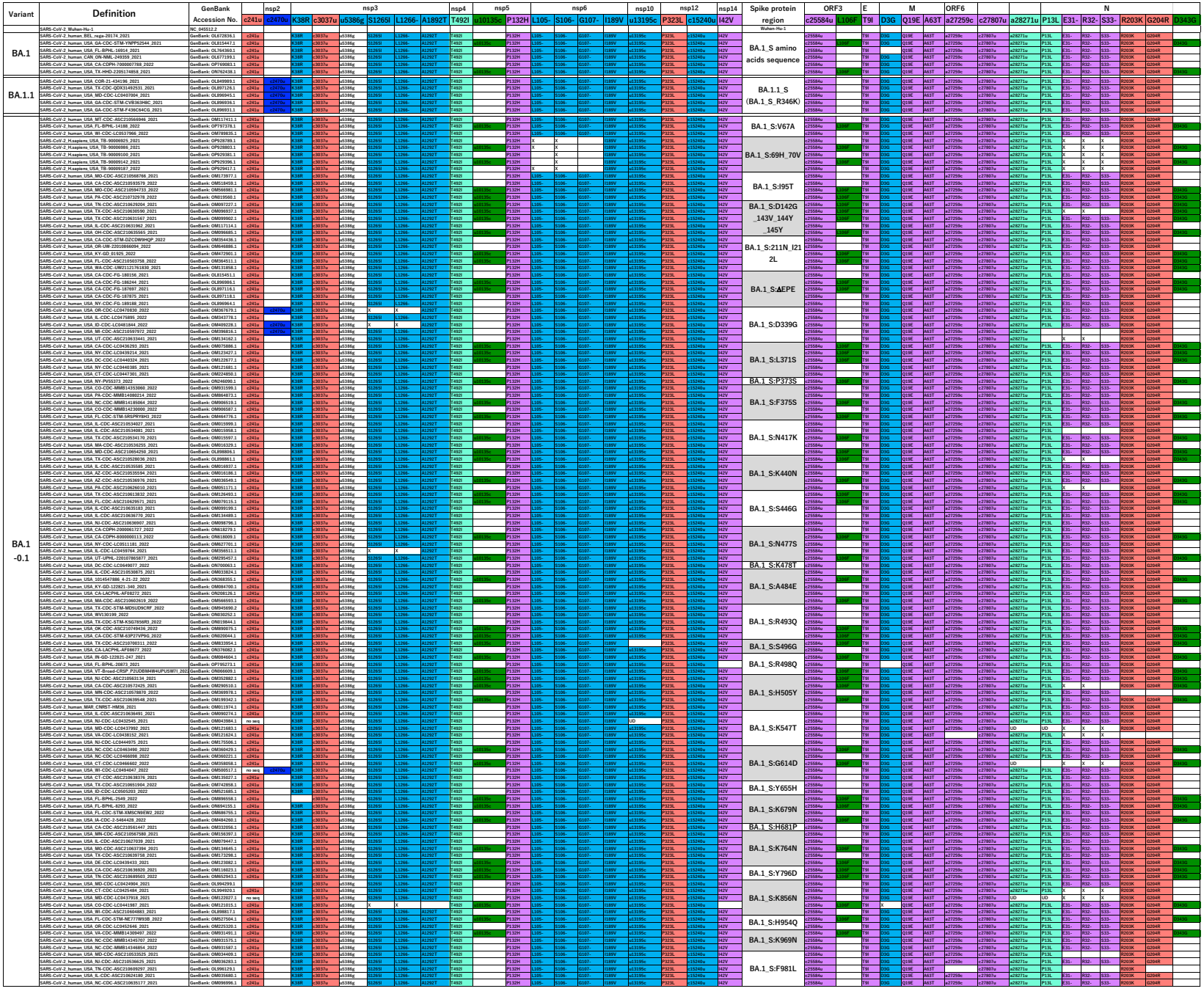

Fig. 4 B

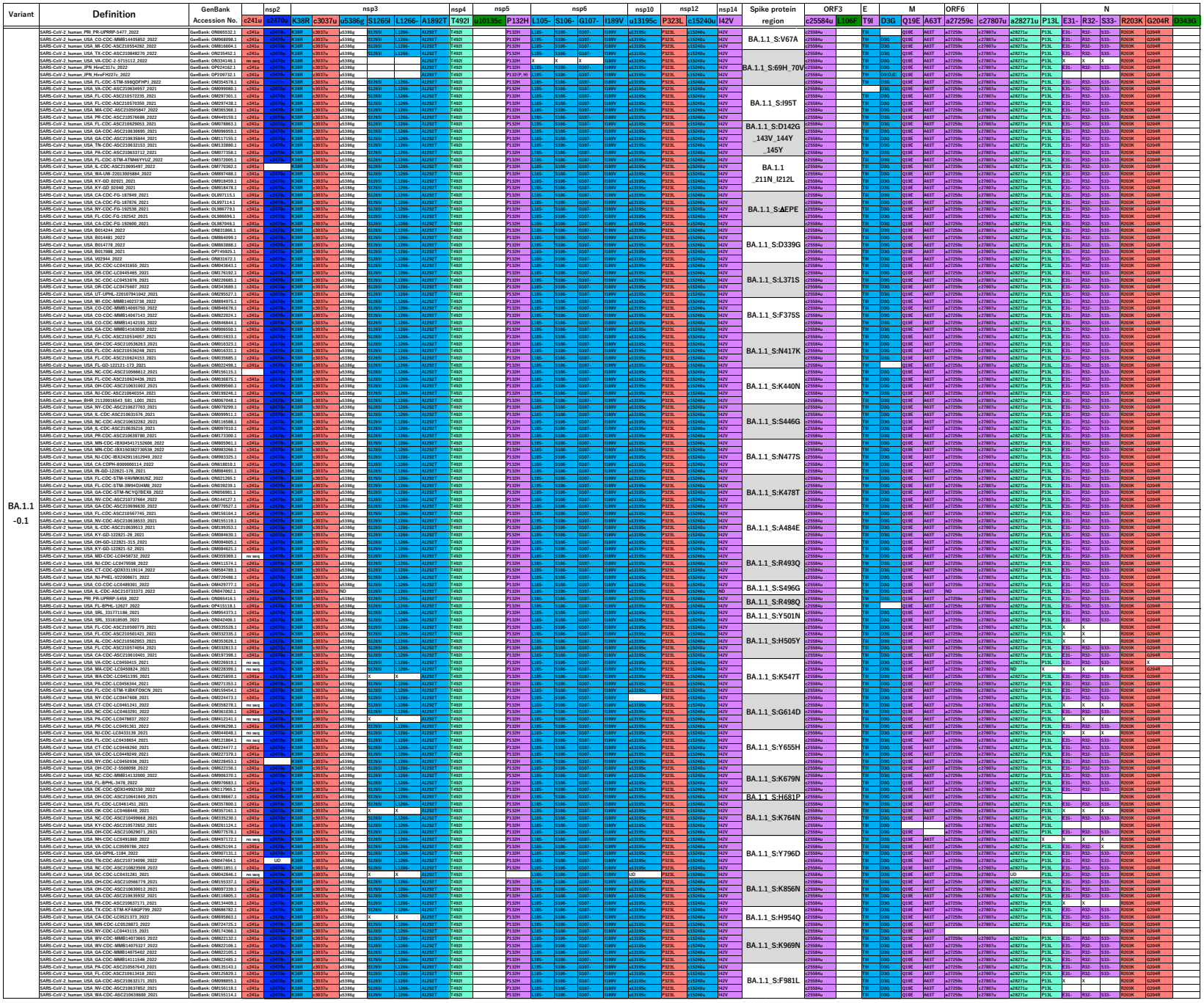

Fig. 5

A

SARS-CoV-2_Omicron_BA1-BA2 recombinant (BA1/2)

Variant	Definition	GenBank Accession No.	Non-synonymous																																																Synonymous			
				deletion[5]					deletion[1]				deletion[2]			deletion[3]			insertion[4]	Receptor-binding domain (RBD) 319 – 541																																		
								A67V	H69-	V70-	T95I	G142D	V143-	Y144-	Y145-	N211I	L212-		215ins. EPE	G339D	R346K	S371L	S373P	S375F				K417N	N440K	G446S	S477N	T478K	E484A	Q493R	G496S	Q498R	N501Y	Y505H	T547K	D614G	H655Y	N679K	P681H	N764K	D796Y	N856K	Q954H	N969K	L981F	Others*	c21595u*	c22792u*	c25000u	Others*
			T19I	L24-	P25-	P26-	A27S					G142D						V213G		G339D		S371F	S373P	S375F	T376A	D405N	R408S	K417N	N440K		S477N	T478K	E484A	Q493R		Q498R	N501Y	Y505H		D614G	H655Y	N679K	P681H	N764K	D796Y		Q954H	N969K						
BA1.1	SARS-CoV-2_human_USA_TX-CDC-QDX31492531_2021	GenBank: OL897126.1						A67V	H69-	V70-	T95I	G142D	V143-	Y144-	Y145-	N211I	L212-		215ins. EPE	G339D	R346K	S371L	S373P	S375F				K417N	N440K	G446S	S477N	T478K	E484A	Q493R	G496S	Q498R	N501Y	Y505H	T547K	D614G	H655Y	N679K	P681H	N764K	D796Y	N856K	Q954H	N969K	L981F				c25000u	
BA2	SARS-CoV-2_human_USA_CA-CDC-FG-229617_2021	GenBank: OM233931.1	T19I	L24-	P25-	P26-	A27S					G142D						V213G		G339D		S371F	S373P	S375F	T376A	D405N	R408S	K417N	N440K		S477N	T478K	E484A	Q493R		Q498R	N501Y	Y505H		D614G	H655Y	N679K	P681H	N764K	D796Y		Q954H	N969K					c25000u	
BA1/2	SARS-CoV-2_human_USA_VA-CDC-LC0464413_2022	GenBank: OM360636.1	T19I					A67V	H69-	V70-	T95I	G142D	V143-	Y144-	Y145-	N211I	L212-		215ins. EPE	G339D		S371L	S373P	S375F				K417N	N440K	G446S	S477N	T478K	E484A	Q493R	G496S	Q498R	N501Y	Y505H	T547K	D614G	H655Y	N679K	P681H	N764K	D796Y	N856K	Q954H	N969K	L981F				c25000u	
	SARS-CoV-2_human_USA_NY-CDC-LC0476274_2022	GenBank: OM410816.1	T19I					A67V	H69-	V70-	T95I	G142D	V143-	Y144-	Y145-	N211I	L212-		215ins. EPE	G339D		S371L	S373P	S375F				K417N	N440K	G446S	S477N	T478K	E484A	Q493R	G496S	Q498R	N501Y	Y505H	T547K	D614G	H655Y	N679K	P681H	N764K	D796Y	N856K	Q954H	N969K	L981F				c25000u	
	SARS-CoV-2_human_USA_AZ-CDC-LC0488280_2022	GenBank: OM429902.1	T19I					A67V	H69-	V70-	T95I	G142D	V143-	Y144-	Y145-	N211I	L212-		215ins. EPE	G339D		S371L	S373P	S375F				K417N	N440K	G446S	S477N	T478K	E484A	Q493R	G496S	Q498R	N501Y	Y505H	T547K	D614G	H655Y	N679K	P681H	N764K	D796Y	N856K	Q954H	N969K	L981F				c25000u	
	SARS-CoV-2_human_USA_WA-CDC-LC0499478_2022	GenBank: OM497964.1	T19I					A67V	H69-	V70-	T95I	G142D	V143-	Y144-	Y145-	N211I	L212-		215ins. EPE	G339D		S371L	S373P	S375F				K417N	N440K	G446S	S477N	T478K	E484A	Q493R	G496S	Q498R	N501Y	Y505H	T547K	D614G	H655Y	N679K	P681H	N764K	D796Y	N856K	Q954H	N969K	L981F				c25000u	c25117u
	SARS-CoV-2_human_USA_MS-CDC-ASC210602041_2022	GenBank: OM565587.1	T19I					A67V	H69-	V70-	T95I	G142D	V143-	Y144-	Y145-	N211I	L212-		215ins. EPE	G339D		S371L	S373P	S375F				K417N	N440K	G446S	S477N	T478K	E484A	Q493R	G496S	Q498R	N501Y	Y505H	T547K	D614G	H655Y	N679K	P681H	N764K	D796Y	N856K	Q954H	N969K	L981F				c25000u	
	SARS-CoV-2_human_USA_NJ-CDC-LC0510764_2022	GenBank: OM628132.1	T19I					A67V	H69-	V70-	T95I	G142D	V143-	Y144-	Y145-	N211I	L212-		215ins. EPE	G339D		S371L	S373P	S375F		D405N	R408S	K417N	N440K	G446S	S477N	T478K	E484A	Q493R	G496S	Q498R	N501Y	Y505H	T547K	D614G	H655Y	N679K	P681H	N764K	D796Y		Q954H	N969K	L981F				c25000u	
	SARS-CoV-2_human_USA_MP-CDC-2-5772902_2022	GenBank: ON549899.1	T19I	L24-	P25-	P26-	A27S	A67V	H69-	V70-	T95I	G142D	V143-	Y144-	Y145-	N211I	L212-		215ins. EPE	G339D	R346K	S371L	S373P	S375F				K417N	N440K	G446S	S477N	T478K	E484A	Q493R	G496S	Q498R	N501Y	Y505H		D614G	H655Y	N679K	P681H	N764K	D796Y	N856K	Q954H	N969K	L981F				c25000u	
	SARS-CoV-2_human_USA_NJ-CDC-LC0592441_2022	GenBank: ON449685.1	T19I	L24-	P25-	P26-	A27S	A67V	H69-	V70-	T95I	G142D	V143-	Y144-	Y145-	N211I	L212-		215ins. EPE	G339D		S371L	S373P	S375F		D405N		K417N	N440K	G446S	S477N	T478K	E484A	Q493R	G496S	Q498R	N501Y	Y505H		D614G	H655Y	N679K	P681H	N764K	D796Y		Q954H	N969K					c25000u	
	SARS-CoV-2_human_USA_FL-CDC-QDX35136213_2022	GenBank: ON176765.1	T19I	L24-	P25-	P26-	A27S	A67V	H69-	V70-		G142D	V143-	Y144-	Y145-	N211I	L212-		215ins. EPE	G339D	R346K	S371L	S373P	S375F			R408S	K417N	N440K		S477N	T478K	E484A	Q493R	G496S	Q498R	N501Y	Y505H		D614G	H655Y	N679K	P681H	N764K	D796Y	N856K	Q954H	N969K	L981F				c25000u	
	SARS-CoV-2_human_USA_PA-CDC-LC0510661_2022	GenBank: OM628094.1	T19I	L24-	P25-	P26-	A27S	A67V	H69-	V70-	T95I	G142D	V143-	Y144-	Y145-	N211I	L212-		215ins. EPE	G339D		S371L	S373P	S375F	T376A	D405N	R408S	K417N	N440K		S477N	T478K	E484A	Q493R	G496S	Q498R	N501Y	Y505H		D614G	H655Y	N679K	P681H	N764K	D796Y		Q954H	N969K					c25000u	
	SARS-CoV-2_human_MWI_MLW000918_2022	GenBank: ON099844.1	T19I	L24-	P25-	P26-	A27S	A67V	H69-	V70-	T95I	G142D	V143-	Y144-	Y145-	N211I	L212-		215ins. EPE	G339D		S371F	S373P	S375F	T376A	D405N	R408S	K417N	N440K		S477N	T478K	E484A	Q493R		Q498R	N501Y	Y505H		D614G	H655Y	N679K	P681H	N764K	D796Y		Q954H	N969K					c25000u	
	SARS-CoV-2_human_USA_MD-CDC-LC0548614_2022	GenBank: OM942313.1	T19I	L24-	P25-	P26-	A27S					G142D	V143-	Y144-	Y145-	N211I	L212-		215ins. EPE	G339D		S371F	S373P	S375F	T376A	D405N	R408S	K417N	N440K		S477N	T478K	E484A	Q493R		Q498R	N501Y	Y505H	T547K	D614G	H655Y	N679K	P681H	N764K	D796Y		Q954H	N969K	L981F				c25000u	
	SARS-CoV-2_human_USA_VT-CDC-LC0584068_2022	GenBank: ON395480.1	T19I	L24-	P25-	P26-	A27S	A67V	H69-	V70-	T95I	G142D	V143-	Y144-	Y145-	N211I	L212-		215ins. EPE	G339D		S371F	S373P	S375F	T376A	D405N	R408S	K417N	N440K		S477N	T478K	E484A	Q493R		Q498R	N501Y	Y505H	T547K	D614G	H655Y	N679K	P681H	N764K	D796Y		Q954H	N969K					c25000u	g25126a
	SARS-CoV-2_human_BHR_22020050752_2022	GenBank: ON171854.1						A67V	H69-	V70-	T95I	G142D	V143-	Y144-	Y145-	N211I	L212-		215ins. EPE	G339D		S371F	S373P	S375F	T376A			K417N	N440K	G446S	S477N	T478K	E484A	Q493R	G496S	Q498R	N501Y	Y505H	T547K	D614G	H655Y	N679K	P681H	N764K	D796Y	N856K	Q954H	N969K	L981F				c25000u	
	SARS-CoV-2_human_BHR_22020083147_2022	GenBank: ON172005.1						A67V	H69-	V70-	T95I	G142D	V143-	Y144-	Y145-	N211I	L212-		215ins. EPE	G339D		S371F	S373P	S375F	T376A			K417N	N440K	G446S	S477N	T478K	E484A	Q493R	G496S	Q498R	N501Y	Y505H	T547K	D614G	H655Y	N679K	P681H	N764K	D796Y	N856K	Q954H	N969K	L981F				c25000u	
	SARS-CoV-2_human_BHR_R45902244162_2022	GenBank: ON076710.1						A67VI108:I1	H69-	V70-	T95I	G142D	V143-	Y144-	Y145-	N211I	L212-		215ins. EPE	G339D		S371F	S373P	S375F	T376A	D405N	R408S	K417N		G446S	S477N	T478K	E484A	Q493R	G496S	Q498R	N501Y	Y505H	T547K	D614G	H655Y	N679K	P681H	N764K	D796Y	N856K	Q954H	N969K	L981F	N81K			c25000u	
	SARS-CoV-2_human_PRI_PR-UPRRP-582_2020	GenBank: ON928946.1						A67V	H69-	V70-	T95I	G142D	V143-	Y144-	Y145-	N211I	L212-		215ins. EPE	G339D		S371F	S373P	S375F	T376A	D405N	R408S	K417N	N440K		S477N	T478K	E484A	Q493R		Q498R	N501Y	Y505H	T547K	D614G	H655Y	N679K	P681H	N764K	D796Y	N856K	Q954H	N969K	L981F				c25000u	
	SARS-CoV-2_human_USA_CO-CDPHE-2102746580_2022	GenBank: OM932113.1						A67V	H69-	V70-	T95I	G142D	V143-	Y144-	Y145-	N211I	L212-	V213G	215ins. EPE	G339D	R346K	S371L	S373P	S375F				K417N	N440K	G446S	S477N	T478K	E484A	Q493R	G496S	Q498R	N501Y	Y505H	T547K	D614G	H655Y	N679K	P681H	N764K	D796Y	N856K	Q954H	N969K	L981F		c21595u		c25000u	
	SARS-CoV-2_human_USA_NC-CDC-LC0549417_2022	GenBank: OM942438.1						A67V	H69-	V70-	T95I	G142D	V143-	Y144-	Y145-	N211I	L212-	V213G	215ins. EPE	G339D	R346K	S371L	S373P	S375F				K417N	N440K	G446S	S477N	T478K	E484A	Q493R	G496S	Q498R	N501Y	Y505H	T547K	D614G	H655Y	N679K	P681H	N764K	D796Y	N856K	Q954H	N969K	L981F				c25000u	a23146g
	SARS-CoV-2_human_USA_NC-CDC-LC0558337_2022	GenBank: OM989528.1						A67V	H69-	V70-	T95I	G142D	V143-	Y144-	Y145-	N211I	L212-	V213G	215ins. EPE	G339D	R346K	S371L	S373P	S375F				K417N	N440K	G446S	S477N	T478K	E484A	Q493R	G496S	Q498R	N501Y	Y505H	T547K	D614G	H655Y	N679K	P681H	N764K	D796Y	N856K	Q954H	N969K	L981F				c25000u	a23146g
	SARS-CoV-2_human_USA_VA-CDC-LC0495278_2022	GenBank: OM499181.1						A67V	H69-	V70-	T95I	G142D	V143-	Y144-	Y145-	N211I	L212-	V213G	215ins. EPE	G339D		S371F	S373P	S375F	T376A	D405N	R408S	K417N	N440K		S477N	T478K	E484A	Q493R		Q498R	N501Y	Y505H		D614G	H655Y	N679K	P681H	N764K	D796Y	N856K	Q954H	N969K	L981F				c25000u	
	SARS-CoV-2_human_USA_NJ-CDC-LC0589728_2022	GenBank: ON414822.1						A67V	H69-	V70-	T95I	G142D	V143-	Y144-	Y145-	N211I	L212-		215ins. EPE	G339D		S371F	S373P	S375F	T376A	D405N	R408S	K417N	N440K		S477N	T478K	E484A	Q493R	G496S	Q498R	N501Y	Y505H	T547K	D614G	H655Y	N679K	P681H	N764K	D796Y	N856K	Q954H	N969K	L981F				c25000u	
	SARS-CoV-2_human_USA_CA-CDC-FG-280689_2022	GenBank: OM878325.1						A67V	H69-	V70-	T95I	G142D	V143-	Y144-	Y145-	N211I	L212-		215ins. EPE	G339D		S371F	S373P	S375F	T376A	D405N	R408S	K417N	N440K	G446S	S477N	T478K	E484A	Q493R	G496S	Q498R	N501Y	Y505H	T547K	D614G	H655Y	N679K	P681H	N764K	D796Y	N856K	Q954H	N969K	L981F			c22792u	c25000u	
	SARS-CoV-2_human_BHR_22970089376_2022	GenBank: ON103067.1						A67V	H69-	V70-	T95I	G142D	V143-	Y144-	Y145-	N211I	L212-		215ins. EPE	G339D	R346K	S371F	S373P	S375F	T376A	D405N	R408S	K417N	N440K	G446S	S477N	T478K	E484A	Q493R	G496S	Q498R	N501Y	Y505H	T547K	D614G	H655Y	N679K	P681H	N764K	D796Y	N856K	Q954H	N969K	L981F				c25000u	
	SARS-CoV-2_human_BHR_22970088641_2022	GenBank: ON103153.1						A67V	H69-	V70-	T95I	G142D	V143-	Y144-	Y145-	N211I	L212-		215ins. EPE	G339D	R346K	S371F	S373P	S375F	T376A	D405N	R408S	K417N	N440K	G446S	S477N	T478K	E484A	Q493R	G496S	Q498R	N501Y	Y505H	T547K	D614G	H655Y	N679K	P681H	N764K	D796Y	N856K	Q954H	N969K	L981F				c25000u	
	SARS-CoV-2_human_BHR_22970059078_2022	GenBank: ON419036.1						A67V	H69-	V70-	T95I	G142D	V143-	Y144-	Y145-	N211I	L212-		215ins. EPE	G339D	R346K	S371F	S373P	S375F	T376A	D405N	R408S	K417N	N440K	G446S	S477N	T478K	E484A	Q493R	G496S	Q498R	N501Y	Y505H	T547K	D614G	H655Y	N679K	P681H	N764K	D796Y	N856K	Q954H	N969K	L981F				c25000u	
	SARS-CoV-2_human_PRI_PR-UPRRP-5813_2022	GenBank: ON928719.1						A67V	H69-	V70-	T95I	G142D	V143-	Y144-	Y145-	N211I	L212-		215ins. EPE	G339D	R346K	S371F	S373P	S375F	T376A	D405N	R408S	K417N	N440K	G446S	S477N	T478K	E484A	Q493R	G496S	Q498R	N501Y	Y505H	T547K	D614G	H655Y	N679K	P681H	N764K	D796Y	N856K	Q954H	N969K	L981F		c21595u	c22792u	c25000u	
	SARS-CoV-2_human_USA_MA-MGB-04990_2022	GenBank: ON337887.1						A67V	H69-	V70-	T95I	G142D	V143-	Y144-	Y145-	N211I	L212-		215ins. EPE	G339D		S371F	S373P	S375F	T376A	D405N	R408S	K417N		G446S	S477N	T478K	E484A	Q493R	G496S	Q498R	N501Y	Y505H	T547K	D614G	H655Y	N679K	P681H	N764K	D796Y	N856K	Q954H	N969K	L981F		c21595u			
	SARS-CoV-2_human_BHR_22020079101_2022	GenBank: ON420444.1						A67V	H69-	V70-	T95I	G142D	V143-	Y144-	Y145-	N211I	L212-		215ins. EPE	G339D		S371F	S373P	S375F	T376A	D405N	R408S	K417N		G446S	S477N	T478K	E484A	Q493R	G496S	Q498R	N501Y	Y505H	T547K	D614G	H655Y	N679K	P681H	N764K	D796Y	N856K	Q954H	N969K	L981F				c25000u	
	SARS-CoV-2_human_BHR_22020048762_2022	GenBank: ON146520.1						A67V	H69-	V70-	T95I	G142D	V143-	Y144-	Y145-	N211I	L212-		215ins. EPE	G339D	R346K	S371F	S373P	S375F	T376A			K417N	N440K	G446S	S477N	T478K	E484A	Q493R	G496S	Q498R	N501Y	Y505H	T547K	D614G	H655Y	N679K	P681H	N764K	D796Y	N856K	Q954H	N969K	L981F				c25000u	
	SARS-CoV-2_human_USA_TX-CDC-QDX32791919_2022	GenBank: OM469541.1						A67V	H69-	V70-	T95I	G142D	V143-	Y144-	Y145-	N211I	L212-		215ins. EPE	G339D		S371L	S373P	S375F	T376A			K417N	N440K	G446S	S477N	T478K	E484A	Q493R	G496S	Q498R	N501Y	Y505H	T547K	D614G	H655Y	N679K	P681H	N764K	D796Y	N856K	Q954H	N969K	L981F				c25000u	
	SARS-CoV-2_human_USA_CT-CDC-QDX33920786_2022	GenBank: OM904085.1						A67V	H69-	V70-	T95I	G142D	V143-	Y144-	Y145-	N211I	L212-		215ins. EPE	G339D		S371L	S373P	S375F	T376A			K417N	N440K	G446S	S477N	T478K	E484A	Q493R	G496S	Q498R	N501Y	Y505H	T547K	D614G	H655Y	N679K	P681H	N764K	D796Y	N856K	Q954H	N969K	L981F				c25000u	
	SARS-CoV-2_human_USA_TX-DSHS-18056_2022	GenBank: ON254531.1						A67V	H69-	V70-	T95I	G142D	V143-	Y144-	Y145-	N211I	L212-		215ins. EPE	G339D		S371L	S373P	S375F	T376A			K417N	N440K	G446S	S477N	T478K	E484A	Q493R	G496S	Q498R	N501Y	Y505H	T547K	D614G	H655Y	N679K	P681H	N764K	D796Y	N856K	Q954H	N969K	L981F				c25000u	g21724a, a23416T
	SARS-CoV-2_human_USA_CA-CDC-FG-283967_2022	GenBank: OM881098.1						A67V	H69-	V70-	T95I	G142D	V143-	Y144-	Y145-	N211I	L212-		215ins. EPE	G339D		S371L	S373P	S375F		D405N	R408S	K417N	N440K	G446S	S477N	T478K	E484A	Q493R	G496S	Q498R	N501Y	Y505H	T547K	D614G	H655Y	N679K	P681H	N764K	D796Y	N856K	Q954H	N969K	L981F				c25000u	
	SARS-CoV-2_human_USA_IL-CDC-LC0582943_2022	GenBank: ON373310.1						A67V	H69-	V70-	T95I	G142D	V143-	Y144-	Y145-	N211I	L212-		215ins. EPE	G339D	R346K	S371L	S373P	S375F		D405N	R408S	K417N	N440K	G446S	S477N	T478K	E484A	Q493R	G496S	Q498R	N501Y	Y505H	T547K	D614G	H655Y	N679K	P681H	N764K	D796Y	N856K	Q954H	N969K					c25000u	c25006u

B

SARS-CoV-2_isolated in Puerto Rico in 2020

Variant	Definition	GenBank Accession No.	T19I	L24-	P25-	P26-	A27S	A67V	H69-	V70-	T95I	G142D	V143-	Y144-	Y145-	N211I	L212-	V213G	215ins. EPE	G339D	R346K	S371L/S371F	S373P	S375F	T376A	D405N	R408S	K417N	N440K	G446S	S477N	T478K	E484A	Q493R	G496S	Q498R	N501Y	Y505H	T547K	D614G	H655Y	N679K	P681H	N764K	D796Y	N856K	Q954H	N969K	L981F	Others*	c21595u*	c22792u*	c25000u	Others*
BA.1.1	SARS-CoV-2_human_PRI_PR-UPRRP-477_2020	GenBank: ON928761.1						A67V	H69-	V70-	T95I	G142D	V143-	Y144-	Y145-	N211I	L212-		215ins. EPE	G339D	R346K	S371L	S373P	S375F				K417N	N440K	G446S	S477N	T478K	E484A	Q493R	G496S	Q498R	N501Y	Y505H	T547K	D614G	H655Y	N679K	P681H	N764K	D796Y	N856K	Q954H	N969K	L981F	V83L	c21595u		c25000u	
	SARS-CoV-2_human_PRI_PR-UPRRP-483_2020	GenBank: ON928660.1						A67V	H69-	V70-	T95I	G142D	V143-	Y144-	Y145-	N211I	L212-		215ins. EPE	G339D	R346K	S371L	S373P	S375F				K417N	N440K	G446S	S477N	T478K	E484A	Q493R	G496S	Q498R	N501Y	Y505H	T547K	D614G	H655Y	N679K	P681H	N764K	D796Y	N856K	Q954H	N969K	L981F		c21595u		c25000u	
	SARS-CoV-2_human_PRI_PR-UPRRP-484_2020	GenBank: ON928794.1						A67V	H69-	V70-	T95I	G142D	V143-	Y144-	Y145-	N211I	L212-		215ins. EPE	G339D	R346K	S371L	S373P	S375F				K417N	N440K	G446S	S477N	T478K	E484A	Q493R	G496S	Q498R	N501Y	Y505H	T547K	D614G	H655Y	N679K	P681H	N764K	D796Y	N856K	Q954H	N969K	L981F		c21595u		c25000u	
	SARS-CoV-2_human_PRI_PR-UPRRP-485_2020	GenBank: ON928762.1						A67V	H69-	V70-	T95I	G142D	V143-	Y144-	Y145-	N211I	L212-		215ins. EPE	G339D	R346K	S371L	S373P	S375F				K417N	N440K	G446S	S477N	T478K	E484A	Q493R	G496S	Q498R	N501Y	Y505H	T547K	D614G	H655Y	N679K	P681H	N764K	D796Y	N856K	Q954H	N969K	L981F		c21595u		c25000u	
	SARS-CoV-2_human_PRI_PR-UPRRP-492_2020	GenBank: ON928848.1						A67V	H69-	V70-	T95I	G142D	V143-	Y144-	Y145-	N211I	L212-		215ins. EPE	G339D	R346K	S371L	S373P	S375F				K417N	N440K	G446S	S477N	T478K	E484A	Q493R	G496S	Q498R	N501Y	Y505H	T547K	D614G	H655Y	N679K	P681H	N764K	D796Y	N856K	Q954H	N969K	L981F		c21595u		c25000u	
	SARS-CoV-2_human_PRI_PR-UPRRP-493_2020	GenBank: ON928741.1						A67V	H69-	V70-	T95I	G142D	V143-	Y144-	Y145-	N211I	L212-		215ins. EPE	G339D	R346K	S371L	S373P	S375F				K417N	N440K	G446S	S477N	T478K	E484A	Q493R	G496S	Q498R	N501Y	Y505H	T547K	D614G	H655Y	N679K	P681H	N764K	D796Y	N856K	Q954H	N969K	L981F		c21595u		c25000u	
	SARS-CoV-2_human_PRI_PR-UPRRP-499_2020	GenBank: ON928918.1						A67V	H69-	V70-	T95I	G142D	V143-	Y144-	Y145-	N211I	L212-		215ins. EPE	G339D	R346K	S371L	S373P	S375F				K417N	N440K	G446S	S477N	T478K	E484A	Q493R	G496S	Q498R	N501Y	Y505H	T547K	D614G	H655Y	N679K	P681H	N764K	D796Y	N856K	Q954H	N969K	L981F		c21595u		c25000u	
	SARS-CoV-2_human_PRI_PR-UPRRP-500_2020	GenBank: ON928680.1						A67V	H69-	V70-	T95I	G142D	V143-	Y144-	Y145-	N211I	L212-		215ins. EPE	G339D	R346K	S371L	S373P	S375F				K417N	N440K	G446S	S477N	T478K	E484A	Q493R	G496S	Q498R	N501Y	Y505H	T547K	D614G	H655Y	N679K	P681H	N764K	D796Y	N856K	Q954H	N969K	L981F		c21595u		c25000u	
	SARS-CoV-2_human_PRI_PR-UPRRP-501_2020	GenBank: ON928975.1						A67V	H69-	V70-	T95I	G142D	V143-	Y144-	Y145-	N211I	L212-		215ins. EPE	G339D	R346K	S371L	S373P	S375F				K417N	N440K	G446S	S477N	T478K	E484A	Q493R	G496S	Q498R	N501Y	Y505H	T547K	D614G	H655Y	N679K	P681H	N764K	D796Y	N856K	Q954H	N969K	L981F		c21595u		c25000u	
	SARS-CoV-2_human_PRI_PR-UPRRP-508_2020	GenBank: ON928949.1						A67V	H69-	V70-	T95I	G142D	V143-	Y144-	Y145-	N211I	L212-		215ins. EPE	G339D	R346K	S371L	S373P	S375F				K417N	N440K	G446S	S477N	T478K	E484A	Q493R	G496S	Q498R	N501Y	Y505H	T547K	D614G	H655Y	N679K	P681H	N764K	D796Y	N856K	Q954H	N969K	L981F		c21595u		c25000u	
	SARS-CoV-2_human_PRI_PR-UPRRP-509_2020	GenBank: ON928673.1						A67V	H69-	V70-	T95I	G142D	V143-	Y144-	Y145-	N211I	L212-		215ins. EPE	G339D	R346K	S371L	S373P	S375F				K417N	N440K	G446S	S477N	T478K	E484A	Q493R	G496S	Q498R	N501Y	Y505H	T547K	D614G	H655Y	N679K	P681H	N764K	D796Y	N856K	Q954H	N969K	L981F		c21595u		c25000u	
	SARS-CoV-2_human_PRI_PR-UPRRP-515_2020	GenBank: ON928865.1						A67V	H69-	V70-	T95I	G142D	V143-	Y144-	Y145-	N211I	L212-		215ins. EPE	G339D	R346K	S371L	S373P	S375F				K417N	N440K	G446S	S477N	T478X	E484A	Q493R	G496S	Q498R	N501Y	Y505H	T547K	D614G	H655Y	N679K	P681H	N764K	D796Y	N856K	Q954H	N969K	L981F		c21595u		c25000u	
	SARS-CoV-2_human_PRI_PR-UPRRP-517_2020	GenBank: ON928716.1						A67V	H69-	V70-	T95I	G142D	V143-	Y144-	Y145-	N211I	L212-		215ins. EPE	G339D	R346K	S371L	S373P	S375F				K417N	N440K	G446S	S477N	T478K	E484A	Q493R	G496S	Q498R	N501Y	Y505H	T547K	D614G	H655Y	N679K	P681H	N764K	D796Y	N856K	Q954H	N969K	L981F		c21595u		c25000u	
	SARS-CoV-2_human_PRI_PR-UPRRP-524_2020	GenBank: ON928663.1						A67V	H69-	V70-	T95I	G142D	V143-	Y144-	Y145-	N211I	L212-		215ins. EPE	G339D	R346K	S371L	S373P	S375F				K417N	N440K	G446S	S477N	T478K	E484A	Q493R	G496S	Q498R	N501Y	Y505H	T547K	D614G	H655Y	N679K	P681H	N764K	D796Y	N856K	Q954H	N969K	L981F				c25000u	
	SARS-CoV-2_human_PRI_PR-UPRRP-525_2020	GenBank: ON928779.1						A67V	H69-	V70-	T95I	G142D	V143-	Y144-	Y145-	N211I	L212-		215ins. EPE	G339D	R346K	S371L	S373P	S375F				K417N	N440K	G446S	S477N	T478K	E484A	Q493R	G496S	Q498R	N501Y	Y505H	T547K	D614G	H655Y	N679K	P681H	N764K	D796Y	N856K	Q954H	N969K	L981F		c21595u		c25000u	
	SARS-CoV-2_human_PRI_PR-UPRRP-532_2020	GenBank: ON928896.1						A67V	H69-	V70-	T95I	G142D	V143-	Y144-	Y145-	N211I	L212-		215ins. EPE	G339D	R346K	S371L	S373P	S375F				K417N	N440K	G446S	S477N	T478K	E484A	Q493R	G496S	Q498R	N501Y	Y505H	T547K	D614G	H655Y	N679K	P681H	N764K	D796Y	N856K	Q954H	N969K	L981F		c21595u		c25000u	
BA.1/2	SARS-CoV-2_human_PRI_PR-UPRRP-582_2020	GenBank: ON928946.1						A67V	H69-	V70-	T95I	G142D	V143-	Y144-	Y145-	N211I	L212-		215ins. EPE	G339D		S371F	S373P	S375F	T376A	D405N	R408S	K417N	N440K		S477N	T478K	E484A	Q493R		Q498R	N501Y	Y505H	T547K	D614G	H655Y	N679K	P681H	N764K	D796Y	N856K	Q954H	N969K	L981F				c25000u	
BA.2 & BA.2-0.1 (K440N)	SARS-CoV-2_human_PRI_PR-UPRRP-278_2020	GenBank: ON928912.1	T19I	L24-	P25-	P26-	A27S					G142D						V213G		G339D		S371F	S373P	S375F	T376A	D405N	R408S	K417N			S477N	T478K	E484A	Q493R		Q498R	N501Y	Y505H		D614G	H655Y	N679K	P681H	N764K	D796Y		Q954H	N969K				c22792u	c25000u	
	SARS-CoV-2_human_PRI_PR-UPRRP-574_2020	GenBank: ON928704.1	T19I	L24-	P25-	P26-	A27S					G142D						V213G		G339D		S371F	S373P	S375F	T376A	D405N	R408S	K417N			S477N	T478K	E484A	Q493R		Q498R	N501Y	Y505H		D614G	H655Y	N679K	P681H	N764K	D796Y		Q954H	N969K		F79S			c25000u	
	SARS-CoV-2_human_PRI_PR-UPRRP-575_2020	GenBank: ON928873.1	T19I	L24-	P25-	P26-	A27S					G142D						V213G		G339D		S371F	S373P	S375F	T376A	D405N	R408S	K417N	N440K		S477N	T478K	E484A	Q493R		Q498R	N501Y	Y505H		D614G	H655Y	N679K	P681H	N764K	D796Y		Q954H	N969K				c22792u	c25000u	
	SARS-CoV-2_human_PRI_PR-UPRRP-576_2020	GenBank: ON928813.1	T19I	L24-	P25-	P26-	A27S					G142D						V213G		G339D		S371F	S373P	S375F	T376A	D405N	R408S	K417N	N440K		S477N	T478K	E484A	Q493R		Q498R	N501Y	Y505H		D614G	H655Y	N679K	P681H	N764K	D796Y		Q954H	N969K					c25000u	
	SARS-CoV-2_human_PRI_PR-UPRRP-579_2020	GenBank: ON928898.1	T19I	L24-	P25-	P26-	A27S					G142D						V213G		G339D		S371F	S373P	S375F	T376A	D405N	R408S	K417N	N440K		S477N	T478K	E484A	Q493R		Q498R	N501Y	Y505H		D614G	H655Y	N679K	P681H	N764K	D796Y		Q954H	N969K					c25000u	
	SARS-CoV-2_human_PRI_PR-UPRRP-581_2020	GenBank: ON928765.1	T19I	L24-	P25-	P26-	A27S					G142D						V213G		G339D		S371F	S373P	S375F	T376A	D405N	R408S	K417N	N440K		S477N	T478K	E484A	Q493R		Q498R	N501Y	Y505H		D614G	H655Y	N679K	P681H	N764K	D796Y		Q954H	N969K					c25000u	c21811u
	SARS-CoV-2_human_PRI_PR-UPRRP-583_2020	GenBank: ON928883.1	T19I	L24-	P25-	P26-	A27S					G142D						V213G		G339D		S371F	S373P	S375F	T376A	D405N	R408S	K417N			S477N	T478K	E484A	Q493R		Q498R	N501Y	Y505H		D614G	H655Y	N679K	P681H	N764K	D796Y		Q954H	N969K				c22792u	c25000u	
	SARS-CoV-2_human_PRI_PR-UPRRP-584_2020	GenBank: ON928957.1	T19I	L24-	P25-	P26-	A27S					G142D						V213G		G339D		S371F	S373P	S375F	T376A	D405N	R408S	K417N			S477N	T478K	E484A	Q493R		Q498R	N501Y	Y505H		D614G	H655Y	N679K	P681H	N764K	D796Y		Q954H	N969K					c25000u	
	SARS-CoV-2_human_PRI_PR-UPRRP-588_2020	GenBank: ON928880.1	T19I	L24-	P25-	P26-	A27S					G142D						V213G		G339D		S371F	S373P	S375F	T376A	D405N	R408S	K417N			S477N	T478K	E484A	Q493R		Q498R	N501Y	Y505H		D614G	H655Y	N679K	P681H	N764K	D796Y		Q954H	N969K					c25000u	c22267u
	SARS-CoV-2_human_PRI_PR-UPRRP-589_2020	GenBank: ON928699.1	T19I	L24-	P25-	P26-	A27S					G142D						V213G		G339D		S371F	S373P	S375F	T376A	D405N	R408S	K417N			S477N	T478K	E484A	Q493R		Q498R	N501Y	Y505H		D614G	H655Y	N679K	P681H	N764K	D796Y		Q954H	N969K		Q613H		c22792u	c25000u	a23767g
	SARS-CoV-2_human_PRI_PR-UPRRP-590_2020	GenBank: ON928724.1	T19I	L24-	P25-	P26-	A27S					G142D					L212S	V213G		G339D		S371F	S373P	S375F	T376A	D405N	R408S	K417N			S477N	T478K	E484A	Q493R		Q498R	N501Y	Y505H		D614G	H655Y	N679K	P681H	N764K	D796Y		Q954H	N969K		L212S, D215E		c22792u	c25000u	c21658u, c24865u
	SARS-CoV-2_human_PRI_PR-UPRRP-591_2020	GenBank: ON928941.1	T19I	L24-	P25-	P26-	A27S					G142D					L212S	V213G		G339D		S371F	S373P	S375F	T376A	D405N	R408S	K417N			S477N	T478K	E484A	Q493R		Q498R	N501Y	Y505H		D614G	H655Y	N679K	P681H	N764K	D796Y		Q954H	N969K		L212S,			c25000u	

Supplemental Figure 1

A

B

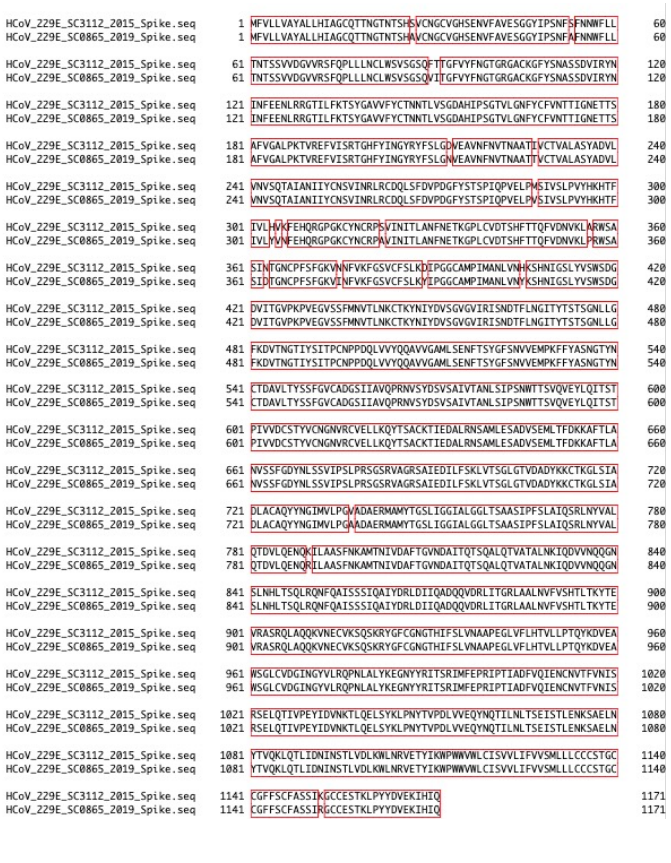

Supplemental Figure 2

Variant	Definition	GenBank Accession No.	T19I	L24-	P25-	P26-	A27S	G142D	V213G	G339D	S371F	S373P	S375F	T376A	D405N	R408S	K417N	N440K	S477N	T478K	E484A	Q493R	Q498R	N501Y	Y505H	D614G	H655Y	N679K	P681H	N764K	D796Y	Q954H	N969K	c22792u*	c25000u	Ouhers*
			Non-synonymous																															Synonymous		
				deletion						Receptor-binding domain (RBD) 319 – 541																										
BA.2	SARS-CoV-2_human_USA_CA-CDC-FG-229617_2021	GenBank: OM233931.1	T19I	L24-	P25-	P26-	A27S	G142D	V213G	G339D	S371F	S373P	S375F	T376A	D405N	R408S	K417N	N440K	S477N	T478K	E484A	Q493R	Q498R	N501Y	Y505H	D614G	H655Y	N679K	P681H	N764K	D796Y	Q954H	N969K		c25000u	
	SARS-CoV-2_human_USA_MA-CDCBI-CRSP_AJSZPA3XZ6CDKXX5_2021	GenBank: OM072551.1	T19I	L24-	P25-	P26-	A27S	G142D	V213G	G339D	S371F	S373P	S375F	T376A	D405N	R408S	K417N	N440K	S477N	T478K	E484A	Q493R	Q498R	N501Y	Y505H	D614G	H655Y	N679K	P681H	N764K	D796Y	Q954H	N969K	c22792u	c25000u	
	SARS-CoV-2_human_USA_MA-CDCBI-CRSP_URIKNCKBF5674VF4_2021	GenBank: OM072822.1	T19I	L24-	P25-	P26-	A27S	G142D	V213G	G339D	S371F	S373P	S375F	T376A	D405N	R408S	K417N	N440K	S477N	T478K	E484A	Q493R	Q498R	N501Y	Y505H	D614G	H655Y	N679K	P681H	N764K	D796Y	Q954H	N969K	c22792u	c25000u	
	SARS-CoV-2_human_USA_WA-S16116_2022	GenBank: OM296922.1	T19I	L24-	P25-	P26-	A27S	G142D	V213G	G339D	S371F	S373P	S375F	T376A	D405N	R408S	K417N	N440K	S477N	T478K	E484A	Q493R	Q498R	N501Y	Y505H	D614G	H655Y	N679K	P681H	N764K	D796Y	Q954H	N969K		c25000u	
BA.2.-0.1	SARS-CoV-2_human_USA_B015025_2022	GenBank: OM863926.1		L24-	P25-	P26-	A27S	G142D	V213G	G339D	S371F	S373P	S375F	T376A	D405N	R408S	K417N	N440K	S477N	T478K	E484A	Q493R	Q498R	N501Y	Y505H	D614G	H655Y	N679K	P681H	N764K	D796Y	Q954H	N969K		c25000u	
	SARS-CoV-2_human_USA_CA-CCPHL-2023_2022	GenBank: ON209298.1		L24-	P25-	P26-	A27S	G142D	V213G	G339D	S371F	S373P	S375F	T376A	D405N	R408S	K417N	N440K	S477N	T478K	E484A	Q493R	Q498R	N501Y	Y505H	D614G	H655Y	N679K	P681H	N764K	D796Y	Q954H	N969K	c22792u	c25000u	a22948g
	SARS-CoV-2_human_USA_CA-CDC-LC0569601_2022	GenBank: ON232806.1		L24-	P25-	P26-	A27S	G142D	V213G	G339D	S371F	S373P	S375F	T376A	D405N	R408S	K417N	N440K	S477N	T478K	E484A	Q493R	Q498R	N501Y	Y505H	D614G	H655Y	N679K	P681H	N764K	D796Y	Q954H	N969K		c25000u	
	SARS-CoV-2_human_USA_CA-LACPHL-AF08976_2022	GenBank: ON421981.1		L24-	P25-	P26-	A27S	G142D	V213G	G339D	S371F	S373P	S375F	T376A	D405N	R408S	K417N	N440K	S477N	T478K	E484A	Q493R	Q498R	N501Y	Y505H	D614G	H655Y	N679K	P681H	N764K	D796Y	Q954H	N969K		c25000u	
	SARS-CoV-2_human_USA_CA-LACPHL-AF10606_2022	GenBank: ON811217.1		L24-	P25-	P26-	A27S	G142D	V213G	G339D	S371F	S373P	S375F	T376A	D405N	R408S	K417N	N440K	S477N	T478K	E484A	Q493R	Q498R	N501Y	Y505H	D614G	H655Y	N679K	P681H	N764K	D796Y	Q954H	N969K		c25000u	
	SARS-CoV-2_human_USA_NY-CDC-LC0518422_2022	GenBank: OM698275.1	T19I					G142D	V213G	G339D	S371F	S373P	S375F	T376A	D405N	R408S	K417N	N440K	S477N	T478K	E484A	Q493R	Q498R	N501Y	Y505H	D614G	H655Y	N679K	P681H	N764K	D796Y	Q954H	N969K		c25000u	c23635u
	SARS-CoV-2_human_IND_17_2021	GenBank: ON052769.1	T19I					G142D	V213G	G339D	S371F	S373P	S375F	T376A	D405N	R408S	K417N	N440K	S477N	T478K	E484A	Q493R	Q498R	N501Y	Y505H	D614G	H655Y	N679K	P681H	N764K	D796Y	Q954H	N969K		c25000u	
	SARS-CoV-2_human_IND_LNHD132_2022	GenBank: ON060006.1	T19I					G142D	V213G	G339D	S371F	S373P	S375F	T376A	D405N	R408S	K417N	N440K	S477N	T478K	E484A	Q493R	Q498R	N501Y	Y505H	D614G	H655Y	N679K	P681H	N764K	D796Y	Q954H	N969K		c25000u	
	SARS-CoV-2_human_IND_LNHD133_2022	GenBank: ON060007.1	T19I					G142D	V213G	G339D	S371F	S373P	S375F	T376A	D405N	R408S	K417N	N440K	S477N	T478K	E484A	Q493R	Q498R	N501Y	Y505H	D614G	H655Y	N679K	P681H	N764K	D796Y	Q954H	N969K		c25000u	
	SARS-CoV-2_human_IND_LNHD135_2022	GenBank: ON060009.1	T19I					G142D	V213G	G339D	S371F	S373P	S375F	T376A	D405N	R408S	K417N	N440K	S477N	T478K	E484A	Q493R	Q498R	N501Y	Y505H	D614G	H655Y	N679K	P681H	N764K	D796Y	Q954H	N969K		c25000u	
	SARS-CoV-2_human_BHR_22020069673_S64_L001_2022	GenBank: OM843171.1	T19I	L24-	P25-	P26-	A27S		V213G	G339D	S371F	S373P	S375F	T376A	D405N	R408S	K417N	N440K	S477N	T478K	E484A	Q493R	Q498R	N501Y	Y505H	D614G	H655Y	N679K	P681H	N764K	D796Y	Q954H	N969K			
	SARS-CoV-2_human_BHR_22020087657_S183_L001_2022	GenBank: OM843276.1	T19I	L24-	P25-	P26-	A27S		V213G	G339D	S371F	S373P	S375F	T376A	D405N	R408S	K417N	N440K	S477N	T478K	E484A	Q493R	Q498R	N501Y	Y505H	D614G	H655Y	N679K	P681H	N764K	D796Y	Q954H	N969K			
	SARS-CoV-2_human_BHR_R1222690028093_S242_L001_2022	GenBank: OM843550.1	T19I	L24-	P25-	P26-	A27S		V213G	G339D	S371F	S373P	S375F	T376A	D405N	R408S	K417N	N440K	S477N	T478K	E484A	Q493R	Q498R	N501Y	Y505H	D614G	H655Y	N679K	P681H	N764K	D796Y	Q954H	N969K			
	SARS-CoV-2_human_BHR_22020089582_S132_L001_2022	GenBank: OM843316.1	T19I	L24-	P25-	P26-	A27S		V213G	G339D	S371F	S373P	S375F	T376A	D405N	R408S	K417N	N440K	S477N	T478K	E484A	Q493R	Q498R	N501Y	Y505H	D614G	H655Y	N679K	P681H	N764K	D796Y	Q954H	N969K			
	SARS-CoV-2_human_BHR_22020090467_S157_L001_2022	GenBank: OM843340.1	T19I	L24-	P25-	P26-	A27S		V213G	G339D	S371F	S373P	S375F	T376A	D405N	R408S	K417N	N440K	S477N	T478K	E484A	Q493R	Q498R	N501Y	Y505H	D614G	H655Y	N679K	P681H	N764K	D796Y	Q954H	N969K			
	SARS-CoV-2_human_USA_NC-CDC-LC0562514_2022	GenBank: ON049267.1	T19I	L24-	P25-	P26-	A27S	G142D		G339D	S371F	S373P	S375F	T376A	D405N	R408S	K417N	N440K	S477N	T478K	E484A	Q493R	Q498R	N501Y	Y505H	D614G	H655Y	N679K	P681H	N764K	D796Y	Q954H	N969K		c25000u	
	SARS-CoV-2_human_USA_FL-CDC-LC0593238_2022	GenBank: ON450720.1	T19I	L24-	P25-	P26-	A27S	G142D		G339D	S371F	S373P	S375F	T376A	D405N	R408S	K417N	N440K	S477N	T478K	E484A	Q493R	Q498R	N501Y	Y505H	D614G	H655Y	N679K	P681H	N764K	D796Y	Q954H	N969K	c22792u	c25000u	c21859u
	SARS-CoV-2_human_USA_MA-CDC-ASC210721152_2022	GenBank: ON250163.1	T19I	L24-	P25-	P26-	A27S	G142D	V213G		S371F	S373P	S375F	T376A	D405N	R408S	K417N	N440K	S477N	T478K	E484A	Q493R	Q498R	N501Y	Y505H	D614G	H655Y	N679K	P681H	N764K	D796Y	Q954H	N969K	c22792u	c25000u	c22945u
	SARS-CoV-2_human_USA_OH-UHTL-2178_2022	GenBank: ON256603.1	T19I	L24-	P25-	P26-	A27S	G142D	V213G		S371F	S373P	S375F	T376A	D405N	R408S	K417N	N440K	S477N	T478K	E484A	Q493R	Q498R	N501Y	Y505H	D614G	H655Y	N679K	P681H	N764K	D796Y	Q954H	N969K		c25000u	
	SARS-CoV-2_human_USA_VSP12938_2022	GenBank: ON480422.1	T19I	L24-	P25-	P26-	A27S	G142D	V213G		S371F	S373P	S375F	T376A	D405N	R408S	K417N	N440K	S477N	T478K	E484A	Q493R	Q498R	N501Y	Y505H	D614G	H655Y	N679K	P681H	N764K	D796Y	Q954H	N969K	c22792u	c25000u	
	SARS-CoV-2_human_USA_NY-CDC-ASC210862593_2022	GenBank: OM888844.1	T19I	L24-	P25-	P26-	A27S	G142D	V213G	G339D		S373P	S375F	T376A	D405N	R408S	K417N	N440K	S477N	T478K	E484A	Q493R	Q498R	N501Y	Y505H	D614G	H655Y	N679K	P681H	N764K	D796Y	Q954H	N969K		c25000u	
	SARS-CoV-2_human_USA_NY-CDC-ASC210822042_2022	GenBank: OM890089.1	T19I	L24-	P25-	P26-	A27S	G142D	V213G	G339D		S373P	S375F	T376A	D405N	R408S	K417N	N440K	S477N	T478K	E484A	Q493R	Q498R	N501Y	Y505H	D614G	H655Y	N679K	P681H	N764K	D796Y	Q954H	N969K		c25000u	c23701u
	SARS-CoV-2_human_USA_OH-UHTL-2087_2022	GenBank: ON009425.2	T19I	L24-	P25-	P26-	A27S	G142D	V213G	G339D		S373P	S375F	T376A	D405N	R408S	K417N	N440K	S477N	T478K	E484A	Q493R	Q498R	N501Y	Y505H	D614G	H655Y	N679K	P681H	N764K	D796Y	Q954H	N969K		c25000u	
	SARS-CoV-2_human_USA_UT-UPHL-220318196385_2022	GenBank: ON082904.1	T19I	L24-	P25-	P26-	A27S	G142D	V213G	G339D		S373P	S375F	T376A	D405N	R408S	K417N	N440K	S477N	T478K	E484A	Q493R	Q498R	N501Y	Y505H	D614G	H655Y	N679K	P681H	N764K	D796Y	Q954H	N969K	c22792u	c25000u	
	SARS-CoV-2_human_USA_MA-CDC-ASC210821187_2022	GenBank: OM901275.1	T19I	L24-	P25-	P26-	A27S	G142D	V213G	G339D		S373P	S375F	T376A	D405N	R408S	K417N	N440K	S477N	T478K	E484A	Q493R	Q498R	N501Y	Y505H	D614G	H655Y	N679K	P681H	N764K	D796Y	Q954H	N969K		c25000u	
	SARS-CoV-2_human_USA_OH-UHTL-1997_2022	GenBank: OM877094.2	T19I	L24-	P25-	P26-	A27S	G142D	V213G	G339D	S371F		S375F	T376A	D405N	R408S	K417N	N440K	S477N	T478K	E484A	Q493R	Q498R	N501Y	Y505H	D614G	H655Y	N679K	P681H	N764K	D796Y	Q954H	N969K		c25000u	
	SARS-CoV-2_human_USA_OH-UHTL-1998_2022	GenBank: OM877095.2	T19I	L24-	P25-	P26-	A27S	G142D	V213G	G339D	S371F		S375F	T376A	D405N	R408S	K417N	N440K	S477N	T478K	E484A	Q493R	Q498R	N501Y	Y505H	D614G	H655Y	N679K	P681H	N764K	D796Y	Q954H	N969K		c25000u	
	SARS-CoV-2_human_USA_OH-UHTL-1999_2022	GenBank: OM877096.2	T19I	L24-	P25-	P26-	A27S	G142D	V213G	G339D	S371F		S375F	T376A	D405N	R408S	K417N	N440K	S477N	T478K	E484A	Q493R	Q498R	N501Y	Y505H	D614G	H655Y	N679K	P681H	N764K	D796Y	Q954H	N969K		c25000u	
	SARS-CoV-2_human_USA_OH-UHTL-2000_2022	GenBank: OM877097.2	T19I	L24-	P25-	P26-	A27S	G142D	V213G	G339D	S371F		S375F	T376A	D405N	R408S	K417N	N440K	S477N	T478K	E484A	Q493R	Q498R	N501Y	Y505H	D614G	H655Y	N679K	P681H	N764K	D796Y	Q954H	N969K		c25000u	
	SARS-CoV-2_human_USA_CO-CDC-MMB15007786_2022	GenBank: ON378542.1	T19I	L24-	P25-	P26-	A27S	G142D	V213G	G339D	S371F	S373P		T376A	D405N	R408S	K417N	N440K	S477N	T478K	E484A	Q493R	Q498R	N501Y	Y505H	D614G	H655Y	N679K	P681H	N764K	D796Y	Q954H	N969K		c25000u	
	SARS-CoV-2_human_USA_CO-CDC-MMB15041240_2022	GenBank: ON389858.1	T19I	L24-	P25-	P26-	A27S	G142D	V213G	G339D	S371F	S373P		T376A	D405N	R408S	K417N	N440K	S477N	T478K	E484A	Q493R	Q498R	N501Y	Y505H	D614G	H655Y	N679K	P681H	N764K	D796Y	Q954H	N969K		c25000u	
	SARS-CoV-2_human_USA_CO-CDC-MMB15051587_2022	GenBank: ON389889.1	T19I	L24-	P25-	P26-	A27S	G142D	V213G	G339D	S371F	S373P		T376A	D405N	R408S	K417N	N440K	S477N	T478K	E484A	Q493R	Q498R	N501Y	Y505H	D614G	H655Y	N679K	P681H	N764K	D796Y	Q954H	N969K		c25000u	c22987u
	SARS-CoV-2_human_USA_CO-CDC-MMB15083993_2022	GenBank: ON390359.1	T19I	L24-	P25-	P26-	A27S	G142D	V213G	G339D	S371F	S373P		T376A	D405N	R408S	K417N	N440K	S477N	T478K	E484A	Q493R	Q498R	N501Y	Y505H	D614G	H655Y	N679K	P681H	N764K	D796Y	Q954H	N969K		c25000u	
	SARS-CoV-2_human_USA_CO-CDC-MMB15083344_2022	GenBank: ON390365.1	T19I	L24-	P25-	P26-	A27S	G142D	V213G	G339D	S371F	S373P		T376A	D405N	R408S	K417N	N440K	S477N	T478K	E484A	Q493R	Q498R	N501Y	Y505H	D614G	H655Y	N679K	P681H	N764K	D796Y	Q954H	N969K		c25000u	
	SARS-CoV-2_human_USA_MN-CDC-IBX999279293948_2022	GenBank: OM936703.1	T19I	L24-	P25-	P26-	A27S	G142D	V213G	G339D	S371F	S373P	S375F		D405N	R408S	K417N	N440K	S477N	T478K	E484A	Q493R	Q498R	N501Y	Y505H	D614G	H655Y	N679K	P681H	N764K	D796Y	Q954H	N969K	c22792u	c25000u	a24433g
	SARS-CoV-2_human_USA_2081650_2022	GenBank: ON352711.1	T19I	L24-	P25-	P26-	A27S	G142D	V213G	G339D	S371F	S373P	S375F		D405N	R408S	K417N	N440K	S477N	T478K	E484A	Q493R	Q498R	N501Y	Y505H	D614G	H655Y	N679K	P681H	N764K	D796Y	Q954H	N969K		c25000u	
	SARS-CoV-2_human_USA_CO-CDC-MMB14969199_2022	GenBank: ON378000.1	T19I	L24-	P25-	P26-	A27S	G142D	V213G	G339D	S371F	S373P	S375F		D405N	R408S	K417N	N440K	S477N	T478K	E484A	Q493R	Q498R	N501Y	Y505H	D614G	H655Y	N679K	P681H	N764K	D796Y	Q954H	N969K		c25000u	
	SARS-CoV-2_human_USA_NY-CDC-QDX35135953_2022	GenBank: ON177702.1	T19I	L24-	P25-	P26-	A27S	G142D	V213G	G339D	S371F	S373P	S375F	T376A		R408S	K417N	N440K	S477N	T478K	E484A	Q493R	Q498R	N501Y	Y505H	D614G	H655Y	N679K	P681H	N764K	D796Y	Q954H	N969K		c25000u	
	SARS-CoV-2_human_USA_UT-UPHL-220403908426_2022	GenBank: ON205494.1	T19I	L24-	P25-	P26-	A27S	G142D	V213G	G339D	S371F	S373P	S375F	T376A		R408S	K417N	N440K	S477N	T478K	E484A	Q493R	Q498R	N501Y	Y505H	D614G	H655Y	N679K	P681H	N764K	D796Y	Q954H	N969K	c22792u	c25000u	a24433g
	SARS-CoV-2_human_USA_CO-CDC-MMB15023382_2022	GenBank: ON378633.1	T19I	L24-	P25-	P26-	A27S	G142D	V213G	G339D	S371F	S373P	S375F	T376A		R408S	K417N	N440K	S477N	T478K	E484A	Q493R	Q498R	N501Y	Y505H	D614G	H655Y	N679K	P681H	N764K	D796Y	Q954H	N969K		c25000u	
	SARS-CoV-2_human_USA_UT-UPHL-220519708663_2022	GenBank: ON617689.1	T19I	L24-	P25-	P26-	A27S	G142D	V213G	G339D	S371F	S373P	S375F	T376A		R408S	K417N	N440K	S477N	T478K	E484A	Q493R	Q498R	N501Y	Y505H	D614G	H655Y	N679K	P681H	N764K	D796Y	Q954H	N969K	c22792u	c25000u	
	SARS-CoV-2_human_USA_NY-PV58389_2022	GenBank: ON619375.1	T19I	L24-	P25-	P26-	A27S	G142D	V213G	G339D	S371F	S373P	S375F	T376A		R408S	K417N	N440K	S477N	T478K	E484A	Q493R	Q498R	N501Y	Y505H	D614G	H655Y	N679K	P681H	N764K	D796Y	Q954H	N969K	c22792u	c25000u	
	SARS-CoV-2_human_USA_GA-GPHL-734_2022	GenBank: OM567618.1	T19I	L24-	P25-	P26-	A27S	G142D	V213G	G339D	S371F	S373P	S375F	T376A	D405N		K417N	N440K	S477N	T478K	E484A	Q493R	Q498R	N501Y	Y505H	D614G	H655Y	N679K	P681H	N764K	D796Y	Q954H	N969K		c25000u	
	SARS-CoV-2_human_USA_MN-CDC-IBX322657542052_2022	GenBank: OM659585.1	T19I	L24-	P25-	P26-	A27S	G142D	V213G	G339D	S371F	S373P	S375F	T376A	D405N		K417N	N440K	S477N	T478K	E484A	Q493R	Q498R	N501Y	Y505H	D614G	H655Y	N679K	P681H	N764K	D796Y	Q954H	N969K		c25000u	
	SARS-CoV-2_human_USA_MA-CDC-ASC210651361_2022	GenBank: OM770913.1	T19I	L24-	P25-	P26-	A27S	G142D	V213G	G339D	S371F	S373P	S375F	T376A	D405N		K417N	N440K	S477N	T478K	E484A	Q493R	Q498R	N501Y	Y505H	D614G	H655Y	N679K	P681H	N764K	D796Y	Q954H	N969K		c25000u	
	SARS-CoV-2_human_USA_MN-CDC-IBX352441390588_2022	GenBank: OM781641.1	T19I	L24-	P25-	P26-	A27S	G142D	V213G	G339D	S371F	S373P	S375F	T376A	D405N		K417N	N440K	S477N	T478K	E484A	Q493R	Q498R	N501Y	Y505H	D614G	H655Y	N679K	P681H	N764K	D796Y	Q954H	N969K		c25000u	
	SARS-CoV-2_human_USA_MN-CDC-IBX076829438540_2022	GenBank: OM805865.1	T19I	L24-	P25-	P26-	A27S	G142D	V213G	G339D	S371F	S373P	S375F	T376A	D405N		K417N	N440K	S477N	T478K	E484A	Q493R	Q498R	N501Y	Y505H	D614G	H655Y	N679K	P681H	N764K	D796Y	Q954H	N969K		c25000u	
	SARS-CoV-2_human_BGD_Laila_918_2022	GenBank: OM533441.1	T19I	L24-	P25-	P26-	A27S	G142D	V213G	G339D	S371F	S373P	S375F	T376A	D405N	R408S		N440K	S477N	T478K	E484A	Q493R	Q498R	N501Y	Y505H	D614G	H655Y	N679K	P681H	N764K	D796Y	Q954H	N969K		c25000u	
	SARS-CoV-2_human_BGD_Laila_923_2022	GenBank: OM533458.1	T19I	L24-	P25-	P26-	A27S	G142D	V213G	G339D	S371F	S373P	S375F	T376A	D405N	R408S		N440K	S477N	T478K	E484A	Q493R	Q498R	N501Y	Y505H	D614G	H655Y	N679K	P681H	N764K	D796Y	Q954H	N969K		c25000u	
	SARS-CoV-2_human_BGD_Laila_872_2022	GenBank: OM570235.1	T19I	L24-	P25-	P26-	A27S	G142D	V213G	G339D	S371F	S373P	S375F	T376A	D405N	R408S		N440K	S477N	T478K	E484A	Q493R	Q498R	N501Y	Y505H	D614G	H655Y	N679K	P681H	N764K	D796Y	Q954H	N969K		c25000u	
	SARS-CoV-2_human_BGD_Laila_887_2022	GenBank: OM570249.1	T19I	L24-	P25-	P26-	A27S	G142D	V213G	G339D	S371F	S373P	S375F	T376A	D405N	R408S		N440K	S477N	T478K	E484A	Q493R	Q498R	N501Y	Y505H	D614G	H655Y	N679K	P681H	N764K	D796Y	Q954H	N969K		c25000u	
	SARS-CoV-2_human_BGD_Laila_879_2022	GenBank: OM570252.1	T19I	L24-	P25-	P26-	A27S	G142D	V213G	G339D	S371F	S373P	S375F	T376A	D405N	R408S		N440K	S477N	T478K	E484A	Q493R	Q498R	N501Y	Y505H	D614G	H655Y	N679K	P681H	N764K	D796Y	Q954H	N969K		c25000u	
	SARS-CoV-2_human_BHR_22120013600_S117_L001_2022	GenBank: OM283320.1	T19I	L24-	P25-	P26-	A27S	G142D	V213G	G339D	S371F	S373P	S375F	T376A	D405N	R408S	K417N		S477N	T478K	E484A	Q493R	Q498R	N501Y	Y505H	D614G	H655Y	N679K	P681H	N764K	D796Y	Q954H	N969K		c25000u	
	SARS-CoV-2_human_BHR_22120021978_S127_L001_2022	GenBank: OM283343.1	T19I	L24-	P25-	P26-	A27S	G142D	V213G	G339D	S371F	S373P	S375F	T376A	D405N	R408S	K417N		S477N	T478K	E484A	Q493R	Q498R	N501Y	Y505H	D614G	H655Y	N679K	P681H	N764K	D796Y	Q954H	N969K		c25000u	
	SARS-CoV-2_human_BHR_22120022463_S77_L001_2022	GenBank: OM283361.1	T19I	L24-	P25-	P26-	A27S	G142D	V213G	G339D	S371F	S373P	S375F	T376A	D405N	R408S	K417N		S477N	T478K	E484A	Q493R	Q498R	N501Y	Y505H	D614G	H655Y	N679K	P681H	N764K	D796Y	Q954H	N969K		c25000u	
	SARS-CoV-2_human_BHR_22120022464_S78_L001_2022	GenBank: OM283362.1	T19I	L24-	P25-	P26-	A27S	G142D	V213G	G339D	S371F	S373P	S375F	T376A	D405N	R408S	K417N		S477N	T478K	E484A	Q493R	Q498R	N501Y	Y505H	D614G	H655Y	N679K	P681H	N764K	D796Y	Q954H	N969K		c25000u	
	SARS-CoV-2_human_BHR_22120022949_S81_L001_2022	GenBank: OM283368.1	T19I	L24-	P25-	P26-	A27S	G142D	V213G	G339D	S371F	S373P	S375F	T376A	D405N	R408S	K417N		S477N	T478K	E484A	Q493R	Q498R	N501Y	Y505H	D614G	H655Y	N679K	P681H	N764K	D796Y	Q954H	N969K		c25000u	
	SARS-CoV-2_human_USA_CA-CDPH-8000000127_2022	GenBank: ON618014.1	T19I	L24-	P25-	P26-	A27S	G142D	V213G	G339D	S371F	S373P	S375F	T376A	D405N	R408S	K417N	N440K		T478K	E484A	Q493R	Q498R	N501Y	Y505H	D614G	H655Y	N679K	P681H	N764K	D796Y	Q954H	N969K		c25000u	
	SARS-CoV-2_human_USA_CA-CDPH-8000000133_2022	GenBank: ON618018.1	T19I	L24-	P25-	P26-	A27S	G142D	V213G	G339D	S371F	S373P	S375F	T376A	D405N	R408S	K417N	N440K		T478K	E484A	Q493R	Q498R	N501Y	Y505H	D614G	H655Y	N679K	P681H	N764K	D796Y	Q954H	N969K		c25000u	c23347u
	SARS-CoV-2_human_USA_CA-CDPH-8000000134_2022	GenBank: ON618019.1	T19I	L24-	P25-	P26-	A27S	G142D	V213G	G339D	S371F	S373P	S375F	T376A	D405N	R408S	K417N	N440K		T478K	E484A	Q493R	Q498R	N501Y	Y505H	D614G	H655Y	N679K	P681H	N764K	D796Y	Q954H	N969K		c25000u	
	SARS-CoV-2_human_USA_CA-CDPH-8000000146_2022	GenBank: ON618027.1	T19I	L24-	P25-	P26-	A27S	G142D	V213G	G339D	S371F	S373P	S375F	T376A	D405N	R408S	K417N	N440K		T478K	E484A	Q493R	Q498R	N501Y	Y505H	D614G	H655Y	N679K	P681H	N764K	D796Y	Q954H	N969K		c25000u	
	SARS-CoV-2_human_USA_CA-CDPH-2000066893_2022	GenBank: ON618363.1	T19I	L24-	P25-	P26-	A27S	G142D	V213G	G339D	S371F	S373P	S375F	T376A	D405N	R408S	K417N	N440K		T478K	E484A	Q493R	Q498R	N501Y	Y505H	D614G	H655Y	N679K	P681H	N764K	D796Y	Q954H	N969K		c25000u	
	SARS-CoV-2_human_USA_IL-CDC-QDX35624690_2022	GenBank: ON311615.1	T19I	L24-	P25-	P26-	A27S	G142D	V213G	G339D	S371F	S373P	S375F	T376A	D405N	R408S	K417N	N440K	S477N	T478K		Q493R	Q498R	N501Y	Y505H	D614G	H655Y	N679K	P681H	N764K	D796Y	Q954H	N969K		c25000u	
	SARS-CoV-2_human_USA_CA-SLOPH-C1219_2022	GenBank: ON383919.1	T19I	L24-	P25-	P26-	A27S	G142D	V213G	G339D	S371F	S373P	S375F	T376A	D405N	R408S	K417N	N440K	S477N	T478K		Q493R	Q498R	N501Y	Y505H	D614G	H655Y	N679K	P681H	N764K	D796Y	Q954H	N969K		c25000u	
	SARS-CoV-2_human_THA_CONI-3664_2022	GenBank: OP579158.1	T19I	L24-	P25-	P26-	A27S	G142D	V213G	G339D	S371F	S373P	S375F	T376A	D405N	R408S	K417N	N440K	S477N	T478K		Q493R	Q498R	N501Y	Y505H	D614G	H655Y	N679K	P681H	N764K	D796Y	Q954H	N969K		c25000u	u24640c
	SARS-CoV-2_human_USA_PA-CDC-QDX38634742_2022	GenBank: OP054411.1	T19I	L24-	P25-	P26-	A27S	G142D	V213G	G339D	S371F	S373P	S375F	T376A	D405N	R408S	K417N	N440K	S477N	T478K		Q493R	Q498R	N501Y	Y505H	D614G	H655Y	N679K	P681H	N764K	D796Y	Q954H	N969K		c25000u	
	SARS-CoV-2_human_USA_TX-CDC-QDX36807347_2022	GenBank: ON633107.1	T19I	L24-	P25-	P26-	A27S	G142D	V213G	G339D	S371F	S373P	S375F	T376A	D405N	R408S	K417N	N440K	S477N	T478K		Q493R	Q498R	N501Y	Y505H	D614G	H655Y	N679K	P681H	N764K	D796Y	Q954H	N969K	c22792u	c25000u	a24619g
	SARS-CoV-2_human_USA_OR-CDC-LC0590554_2022	GenBank: ON414693.1	T19I	L24-	P25-	P26-	A27S	G142D	V213G	G339D	S371F	S373P	S375F	T376A	D405N	R408S	K417N	N440K	S477N	T478K	E484A		Q498R	N501Y	Y505H	D614G	H655Y	N679K	P681H	N764K	D796Y	Q954H	N969K		c25000u	c24865u
	SARS-CoV-2_human_USA_FL-CDC-STM-9ETNSYQ68_2022	GenBank: ON422887.1	T19I	L24-	P25-	P26-	A27S	G142D	V213G	G339D	S371F	S373P	S375F	T376A	D405N	R408S	K417N	N440K	S477N	T478K	E484A		Q498R	N501Y	Y505H	D614G	H655Y	N679K	P681H	N764K	D796Y	Q954H	N969K		c25000u	
	SARS-CoV-2_human_USA_E8DAF5E01C0_2022	GenBank: OP364296.1	T19I	L24-	P25-	P26-	A27S	G142D	V213G	G339D	S371F	S373P	S375F	T376A	D405N	R408S	K417N	N440K	S477N	T478K	E484A		Q498R	N501Y	Y505H	D614G	H655Y	N679K	P681H	N764K	D796Y	Q954H	N969K		c25000u	
	SARS-CoV-2_human_USA_TMCL-022A Nasal Swab_2022	GenBank: OP629673.1	T19I	L24-	P25-	P26-	A27S	G142D	V213G	G339D	S371F	S373P	S375F	T376A	D405N	R408S	K417N	N440K	S477N	T478K	E484A		Q498R	N501Y	Y505H	D614G	H655Y	N679K	P681H	N764K	D796Y	Q954H	N969K		c25000u	
	SARS-CoV-2_human_USA_CA-CDC-QDX35734313_2022	GenBank: ON363097.1	T19I	L24-	P25-	P26-	A27S	G142D	V213G	G339D	S371F	S373P	S375F	T376A	D405N	R408S	K417N	N440K	S477N	T478K	E484A	Q493R		N501Y	Y505H	D614G	H655Y	N679K	P681H	N764K	D796Y	Q954H	N969K	c22792u	c25000u	
	SARS-CoV-2_human_NZL_22CH3603_2022	GenBank: OP633561.1	T19I	L24-	P25-	P26-	A27S	G142D	V213G	G339D	S371F	S373P	S375F	T376A	D405N	R408S	K417N	N440K	S477N	T478K	E484A	Q493R		N501Y	Y505H	D614G	H655Y	N679K	P681H	N764K	D796Y	Q954H	N969K		c25000u	
	SARS-CoV-2_human_USA_CA-CDC-QDX35974755_2022	GenBank: ON458445.1	T19I	L24-	P25-	P26-	A27S	G142D	V213G	G339D	S371F	S373P	S375F	T376A	D405N	R408S	K417N	N440K	S477N	T478K	E484A	Q493R		N501Y	Y505H	D614G	H655Y	N679K	P681H	N764K	D796Y	Q954H	N969K		c25000u	
	SARS-CoV-2_human_USA_NJ-CDC-LC0630974_2022	GenBank: ON592247.1	T19I	L24-	P25-	P26-	A27S	G142D	V213G	G339D	S371F	S373P	S375F	T376A	D405N	R408S	K417N	N440K	S477N	T478K	E484A	Q493R		N501Y	Y505H	D614G	H655Y	N679K	P681H	N764K	D796Y	Q954H	N969K		c25000u	
	SARS-CoV-2_human_USA_NY-CDC-QDX36604947_2022	GenBank: ON549687.1	T19I	L24-	P25-	P26-	A27S	G142D	V213G	G339D	S371F	S373P	S375F	T376A	D405N	R408S	K417N	N440K	S477N	T478K	E484A	Q493R		N501Y	Y505H	D614G	H655Y	N679K	P681H	N764K	D796Y	Q954H	N969K		c25000u	
	SARS-CoV-2_human_USA_MA-Broad-CRSP_RONTL6TVQ6F4W7SU_2022	GenBank: ON067040.1	T19I	L24-	P25-	P26-	A27S	G142D	V213G	G339D	S371F	S373P	S375F	T376A	D405N	R408S	K417N	N440K	S477N	T478K	E484A	Q493R	Q498R		Y505H	D614G	H655Y	N679K	P681H	N764K	D796Y	Q954H	N969K		c25000u	
	SARS-CoV-2_human_USA_NY-Broad-CRSP_W5RRSQYSNEU2CTCC_2022	GenBank: ON199452.1	T19I	L24-	P25-	P26-	A27S	G142D	V213G	G339D	S371F	S373P	S375F	T376A	D405N	R408S	K417N	N440K	S477N	T478K	E484A	Q493R	Q498R		Y505H	D614G	H655Y	N679K	P681H	N764K	D796Y	Q954H	N969K		c25000u	
	SARS-CoV-2_human_USA_MA-Broad-CRSP_HI2VSRB3HJJCYJLN_2022	GenBank: ON200331.1	T19I	L24-	P25-	P26-	A27S	G142D	V213G	G339D	S371F	S373P	S375F	T376A	D405N	R408S	K417N	N440K	S477N	T478K	E484A	Q493R	Q498R		Y505H	D614G	H655Y	N679K	P681H	N764K	D796Y	Q954H	N969K	c22792u	c25000u	
	SARS-CoV-2_human_USA_MA-Broad-CRSP_OTZ2XP3IC3O2MGXT_2022	GenBank: ON200438.1	T19I	L24-	P25-	P26-	A27S	G142D	V213G	G339D	S371F	S373P	S375F	T376A	D405N	R408S	K417N	N440K	S477N	T478K	E484A	Q493R	Q498R		Y505H	D614G	H655Y	N679K	P681H	N764K	D796Y	Q954H	N969K		c25000u	
	SARS-CoV-2_human_USA_VT-Broad-CRSP_BASF6SBPTLBI5WS5_2022	GenBank: ON321116.1	T19I	L24-	P25-	P26-	A27S	G142D	V213G	G339D	S371F	S373P	S375F	T376A	D405N	R408S	K417N	N440K	S477N	T478K	E484A	Q493R	Q498R		Y505H	D614G	H655Y	N679K	P681H	N764K	D796Y	Q954H	N969K		c25000u	
	SARS-CoV-2_human_USA_CA-CDC-ASC210859265_2022	GenBank: OM861064.1	T19I	L24-	P25-	P26-	A27S	G142D	V213G	G339D	S371F	S373P	S375F	T376A	D405N	R408S	K417N	N440K	S477N	T478K	E484A	Q493R	Q498R	N501Y		D614G	H655Y	N679K	P681H	N764K	D796Y	Q954H	N969K		c25000u	
	SARS-CoV-2_human_USA_FL-CDC-ASC210731143_2022	GenBank: OM969592.1	T19I	L24-	P25-	P26-	A27S	G142D	V213G	G339D	S371F	S373P	S375F	T376A	D405N	R408S	K417N	N440K	S477N	T478K	E484A	Q493R	Q498R	N501Y		D614G	H655Y	N679K	P681H	N764K	D796Y	Q954H	N969K		c25000u	
	SARS-CoV-2_human_USA_CA-CDC-ASC210757440_2022	GenBank: ON019120.1	T19I	L24-	P25-	P26-	A27S	G142D	V213G	G339D	S371F	S373P	S375F	T376A	D405N	R408S	K417N	N440K	S477N	T478K	E484A	Q493R	Q498R	N501Y		D614G	H655Y	N679K	P681H	N764K	D796Y	Q954H	N969K		c25000u	
	SARS-CoV-2_human_USA_NY-PBRI-22M007_2022	GenBank: ON221860.1	T19I	L24-	P25-	P26-	A27S	G142D	V213G	G339D	S371F	S373P	S375F	T376A	D405N	R408S	K417N	N440K	S477N	T478K	E484A	Q493R	Q498R	N501Y		D614G	H655Y	N679K	P681H	N764K	D796Y	Q954H	N969K		c25000u	
	SARS-CoV-2_human_USA_NY-PBRI-22M008_2022	GenBank: ON221861.1	T19I	L24-	P25-	P26-	A27S	G142D	V213G	G339D	S371F	S373P	S375F	T376A	D405N	R408S	K417N	N440K	S477N	T478K	E484A	Q493R	Q498R	N501Y		D614G	H655Y	N679K	P681H	N764K	D796Y	Q954H	N969K		c25000u	
	SARS-CoV-2_human_USA_TX-CDC-ASC210858963_2022	GenBank: OM861619.1	T19I	L24-	P25-	P26-	A27S	G142D	V213G	G339D	S371F	S373P	S375F	T376A	D405N	R408S	K417N	N440K	S477N	T478K	E484A	Q493R	Q498R	N501Y	Y505H		H655Y	N679K	P681H	N764K	D796Y	Q954H	N969K		c25000u	
	SARS-CoV-2_human_USA_PA-CDC-LC0564604_2022	GenBank: ON091288.1	T19I	L24-	P25-	P26-	A27S	G142D	V213G	G339D	S371F	S373P	S375F	T376A	D405N	R408S	K417N	N440K	S477N	T478K	E484A	Q493R	Q498R	N501Y	Y505H		H655Y	N679K	P681H	N764K	D796Y	Q954H	N969K		c25000u	
	SARS-CoV-2_human_USA_CT-CDC-LC0566727_2022	GenBank: ON151370.1	T19I	L24-	P25-	P26-	A27S	G142D	V213G	G339D	S371F	S373P	S375F	T376A	D405N	R408S	K417N	N440K	S477N	T478K	E484A	Q493R	Q498R	N501Y	Y505H		H655Y	N679K	P681H	N764K	D796Y	Q954H	N969K		c25000u	
	SARS-CoV-2_human_USA_NJ-CDC-LC0569045_2022	GenBank: ON233850.1	T19I	L24-	P25-	P26-	A27S	G142D	V213G	G339D	S371F	S373P	S375F	T376A	D405N	R408S	K417N	N440K	S477N	T478K	E484A	Q493R	Q498R	N501Y	Y505H		H655Y	N679K	P681H	N764K	D796Y	Q954H	N969K		c25000u	
	SARS-CoV-2_human_USA_CT-CDC-ASC210849642_2022	GenBank: ON236456.1	T19I	L24-	P25-	P26-	A27S	G142D	V213G	G339D	S371F	S373P	S375F	T376A	D405N	R408S	K417N	N440K	S477N	T478K	E484A	Q493R	Q498R	N501Y	Y505H		H655Y	N679K	P681H	N764K	D796Y	Q954H	N969K		c25000u	
	SARS-CoV-2_human_USA_CT-CDC-LC0575807_2022	GenBank: ON296711.1	T19I	L24-	P25-	P26-	A27S	G142D	V213G	G339D	S371F	S373P	S375F	T376A	D405N	R408S	K417N	N440K	S477N	T478K	E484A	Q493R	Q498R	N501Y	Y505H	D614G		N679K	P681H	N764K	D796Y	Q954H	N969K	c22792u	c25000u	
	SARS-CoV-2_human_USA_NY-CDC-LC0610786_2022	GenBank: ON535443.1	T19I	L24-	P25-	P26-	A27S	G142D	V213G	G339D	S371F	S373P	S375F	T376A	D405N	R408S	K417N	N440K	S477N	T478K	E484A	Q493R	Q498R	N501Y	Y505H	D614G		N679K	P681H	N764K	D796Y	Q954H	N969K	c22792u	c25000u	a23989g; u23047c
	SARS-CoV-2_human_USA_NY-CDC-LC0642966_2022	GenBank: ON624524.1	T19I	L24-	P25-	P26-	A27S	G142D	V213G	G339D	S371F	S373P	S375F	T376A	D405N	R408S	K417N	N440K	S477N	T478K	E484A	Q493R	Q498R	N501Y	Y505H	D614G		N679K	P681H	N764K	D796Y	Q954H	N969K		c25000u	
	SARS-CoV-2_human_USA_NJ-CDC-LC0583804_2022	GenBank: ON377450.1	T19I	L24-	P25-	P26-	A27S	G142D	V213G	G339D	S371F	S373P	S375F	T376A	D405N	R408S	K417N	N440K	S477N	T478K	E484A	Q493R	Q498R	N501Y	Y505H	D614G		N679K	P681H	N764K	D796Y	Q954H	N969K		c25000u	u24346c
	SARS-CoV-2_human_USA_DC-CDC-LC0587755_2022	GenBank: ON397268.1	T19I	L24-	P25-	P26-	A27S	G142D	V213G	G339D	S371F	S373P	S375F	T376A	D405N	R408S	K417N	N440K	S477N	T478K	E484A	Q493R	Q498R	N501Y	Y505H	D614G		N679K	P681H	N764K	D796Y	Q954H	N969K		c25000u	
	SARS-CoV-2_human_USA_NJ-PHEL-V22016186_2022	GenBank: ON239032.1	T19I	L24-	P25-	P26-	A27S	G142D	V213G	G339D	S371F	S373P	S375F	T376A	D405N	R408S	K417N	N440K	S477N	T478K	E484A	Q493R	Q498R	N501Y	Y505H	D614G	H655Y		P681H	N764K	D796Y	Q954H	N969K		c25000u	c21811u; c21952u
	SARS-CoV-2_human_USA_WA-CDC-LC0581940_2022	GenBank: ON373649.1	T19I	L24-	P25-	P26-	A27S	G142D	V213G	G339D	S371F	S373P	S375F	T376A	D405N	R408S	K417N	N440K	S477N	T478K	E484A	Q493R	Q498R	N501Y	Y505H	D614G	H655Y		P681H	N764K	D796Y	Q954H	N969K	c22792u	c25000u	
	SARS-CoV-2_human_USA_CA-CDC-STM-Q8JDYJ7WW_2022	GenBank: ON481637.1	T19I	L24-	P25-	P26-	A27S	G142D	V213G	G339D	S371F	S373P	S375F	T376A	D405N	R408S	K417N	N440K	S477N	T478K	E484A	Q493R	Q498R	N501Y	Y505H	D614G	H655Y		P681H	N764K	D796Y	Q954H	N969K		c25000u	
	SARS-CoV-2_human_USA_MD-CDC-LC0651160_2022	GenBank: ON701163.1	T19I	L24-	P25-	P26-	A27S	G142D	V213G	G339D	S371F	S373P	S375F	T376A	D405N	R408S	K417N	N440K	S477N	T478K	E484A	Q493R	Q498R	N501Y	Y505H	D614G	H655Y		P681H	N764K	D796Y	Q954H	N969K	c22792u	c25000u	a22753u
	SARS-CoV-2_human_USA_MI-CDC-ASC210729927_2022	GenBank: OM948079.1	T19I	L24-	P25-	P26-	A27S	G142D	V213G	G339D	S371F	S373P	S375F	T376A	D405N	R408S	K417N	N440K	S477N	T478K	E484A	Q493R	Q498R	N501Y	Y505H	D614G	H655Y		P681H	N764K	D796Y	Q954H	N969K		c25000u	
	SARS-CoV-2_human_USA_UT-UPHL-220417292921_2022	GenBank: ON312677.1	T19I	L24-	P25-	P26-	A27S	G142D	V213G	G339D	S371F	S373P	S375F	T376A	D405N	R408S	K417N	N440K	S477N	T478K	E484A	Q493R	Q498R	N501Y	Y505H	D614G	H655Y	N679K	P681H		D796Y	Q954H	N969K		c25000u	c23635u
	SARS-CoV-2_human_USA_NC-CDC-LC0577859_2022	GenBank: ON349263.1	T19I	L24-	P25-	P26-	A27S	G142D	V213G	G339D	S371F	S373P	S375F	T376A	D405N	R408S	K417N	N440K	S477N	T478K	E484A	Q493R	Q498R	N501Y	Y505H	D614G	H655Y	N679K	P681H		D796Y	Q954H	N969K		c25000u	
	SARS-CoV-2_human_USA_DC-CDC-LC0583490_2022	GenBank: ON377487.1	T19I	L24-	P25-	P26-	A27S	G142D	V213G	G339D	S371F	S373P	S375F	T376A	D405N	R408S	K417N	N440K	S477N	T478K	E484A	Q493R	Q498R	N501Y	Y505H	D614G	H655Y	N679K	P681H		D796Y	Q954H	N969K	c22792u	c25000u	
	SARS-CoV-2_human_USA_VA-CDC-LC0583763_2022	GenBank: ON377609.1	T19I	L24-	P25-	P26-	A27S	G142D	V213G	G339D	S371F	S373P	S375F	T376A	D405N	R408S	K417N	N440K	S477N	T478K	E484A	Q493R	Q498R	N501Y	Y505H	D614G	H655Y	N679K	P681H		D796Y	Q954H	N969K		c25000u	
	SARS-CoV-2_human_USA_VA-CDC-LC0558906_2022	GenBank: OM989887.1	T19I	L24-	P25-	P26-	A27S	G142D	V213G	G339D	S371F	S373P	S375F	T376A	D405N	R408S	K417N	N440K	S477N	T478K	E484A	Q493R	Q498R	N501Y	Y505H	D614G	H655Y	N679K	P681H		D796Y	Q954H	N969K		c25000u	
	SARS-CoV-2_human_BGD_Laila_900_2022	GenBank: OM638574.1	T19I	L24-	P25-	P26-	A27S	G142D	V213G	G339D	S371F	S373P	S375F	T376A	D405N	R408S	K417N	N440K	S477N	T478K	E484A	Q493R	Q498R	N501Y	Y505H	D614G	H655Y	N679K	P681H	N764K		Q954H	N969K		c25000u	
	SARS-CoV-2_human_USA_MA-CDC-ASC210751149_2022	GenBank: OM911616.1	T19I	L24-	P25-	P26-	A27S	G142D	V213G	G339D	S371F	S373P	S375F	T376A	D405N	R408S	K417N	N440K	S477N	T478K	E484A	Q493R	Q498R	N501Y	Y505H	D614G	H655Y	N679K	P681H	N764K		Q954H	N969K		c25000u	
	SARS-CoV-2_human_BHR_470028530_2022	GenBank: OM988767.1	T19I	L24-	P25-	P26-	A27S	G142D	V213G	G339D	S371F	S373P	S375F	T376A	D405N	R408S	K417N	N440K	S477N	T478K	E484A	Q493R	Q498R	N501Y	Y505H	D614G	H655Y	N679K	P681H	N764K		Q954H	N969K		c25000u	
	SARS-CoV-2_human_USA_KS-CDC-ASC210757836_2022	GenBank: ON019770.1	T19I	L24-	P25-	P26-	A27S	G142D	V213G	G339D	S371F	S373P	S375F	T376A	D405N	R408S	K417N	N440K	S477N	T478K	E484A	Q493R	Q498R	N501Y	Y505H	D614G	H655Y	N679K	P681H	N764K		Q954H	N969K		c25000u	c24023u
	SARS-CoV-2_human_BHR_500109885_2022	GenBank: OM988769.1	T19I	L24-	P25-	P26-	A27S	G142D	V213G	G339D	S371F	S373P	S375F	T376A	D405N	R408S	K417N	N440K	S477N	T478K	E484A	Q493R	Q498R	N501Y	Y505H	D614G	H655Y	N679K	P681H	N764K		Q954H	N969K		c25000u	c24382u
	SARS-CoV-2_human_USA_NC-CDC-LC0598357_2022	GenBank: ON468158.1	T19I	L24-	P25-	P26-	A27S	G142D	V213G	G339D	S371F	S373P	S375F	T376A	D405N	R408S	K417N	N440K	S477N	T478K	E484A	Q493R	Q498R	N501Y	Y505H	D614G	H655Y	N679K	P681H	N764K	D796Y		N969K		c25000u	
	SARS-CoV-2_human_USA_NC-CDC-LC0636034_2022	GenBank: ON608924.1	T19I	L24-	P25-	P26-	A27S	G142D	V213G	G339D	S371F	S373P	S375F	T376A	D405N	R408S	K417N	N440K	S477N	T478K	E484A	Q493R	Q498R	N501Y	Y505H	D614G	H655Y	N679K	P681H	N764K	D796Y		N969K	c22792u	c25000u	
	SARS-CoV-2_human_USA_OH-UHTL-2312_2022	GenBank: ON604965.1	T19I	L24-	P25-	P26-	A27S	G142D	V213G	G339D	S371F	S373P	S375F	T376A	D405N	R408S	K417N	N440K	S477N	T478K	E484A	Q493R	Q498R	N501Y	Y505H	D614G	H655Y	N679K	P681H	N764K	D796Y		N969K		c25000u	
	SARS-CoV-2_human_USA_CA-CDC-LC0617566_2022	GenBank: ON535763.1	T19I	L24-	P25-	P26-	A27S	G142D	V213G	G339D	S371F	S373P	S375F	T376A	D405N	R408S	K417N	N440K	S477N	T478K	E484A	Q493R	Q498R	N501Y	Y505H	D614G	H655Y	N679K	P681H	N764K	D796Y		N969K		c25000u	
	SARS-CoV-2_human_USA_CO-CDC-MMB14986462_2022	GenBank: ON378227.1	T19I	L24-	P25-	P26-	A27S	G142D	V213G	G339D	S371F	S373P	S375F	T376A	D405N	R408S	K417N	N440K	S477N	T478K	E484A	Q493R	Q498R	N501Y	Y505H	D614G	H655Y	N679K	P681H	N764K	D796Y	Q954H		c22792u	c25000u	c22572u
	SARS-CoV-2_human_USA_GA-CDC-MMB14986912_2022	GenBank: ON378238.1	T19I	L24-	P25-	P26-	A27S	G142D	V213G	G339D	S371F	S373P	S375F	T376A	D405N	R408S	K417N	N440K	S477N	T478K	E484A	Q493R	Q498R	N501Y	Y505H	D614G	H655Y	N679K	P681H	N764K	D796Y	Q954H		c22792u	c25000u	
	SARS-CoV-2_human_USA_VA-CDC-LC0673698_2022	GenBank: ON728470.1	T19I	L24-	P25-	P26-	A27S	G142D	V213G	G339D	S371F	S373P	S375F	T376A	D405N	R408S	K417N	N440K	S477N	T478K	E484A	Q493R	Q498R	N501Y	Y505H	D614G	H655Y	N679K	P681H	N764K	D796Y	Q954H		c22792u	c25000u	

Supplemental Figure 3

A

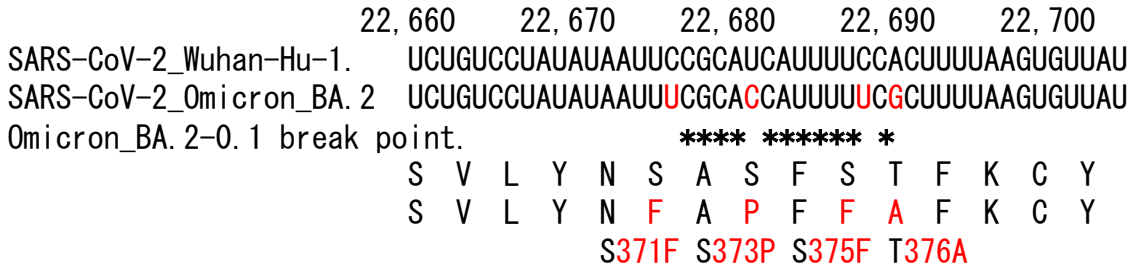

B